Invited Review

Transient landscape and stratigraphic responses to drainage integration in the actively extending central Italian Apennines

Anneleen H. Geurts [a,*], Alexander C. Whittaker [b], Rob L. Gawthorpe [a], Patience A. Cowie [a]

[a] Department of Earth Science, University of Bergen, Bergen, Norway
[b] Department of Earth Science and Engineering, Royal School of Mines, Imperial College, London, UK

ABSTRACT

Drainage networks in continental rifts are generally reported as dynamic features that produce transitions between endorheic and exorheic conditions. While this is of major importance for landscape development, sediment dispersal, and basin stratigraphy, the controls of drainage network evolution across an array of normal fault bounded basins are still not well understood. In this study we use the central Italian Apennines – an area that has been affected by active normal faulting and regional uplift over the last ~3 Myrs – to determine the controls on drainage network evolution and its impact on transient landscape evolution and basin stratigraphy. We compile previously published stratigraphic and fault-related data with new geomorphological constraints for the Aterno River system (~1300 km^2), for which a wealth of data has been collected following the destructive L'Aquila earthquake in 2009. We use this compilation to demonstrate how the different basins along the river system were initially isolated during the Early Pleistocene but became fluvially integrated with one another and the Adriatic coast between ca. 1.2 and 0.65 Ma. We conclude that the spatial and temporal pattern of drainage integration is mostly explained by a long-term increase in sediment and water supply relative to basin subsidence due to the Early to Middle Pleistocene climatic transition, the progressive increase in fault-related topography, and the transport of sediment and water down-system as drainage integration occurred. Overall we conclude that rates of sedimentation and basin subsidence in the central Apennines are well-matched, allowing tipping points between over- and under-filled conditions to be easily reached. We also show that consecutive drainage integration events produce discrete waves of river incision and terrace formation, and conclude that drainage integration is of major importance, at least equivalent to tectonics and climate, in controlling transient landscape evolution and rift basin stratigraphy.

Contents

* Corresponding author.
    E-mail address: Anneleen.Geurts@uib.no (A.H. Geurts).

1. Introduction

Extensional basins in continental rifts commonly go through both phases of internal (endorheic) and external (exorheic) drainage related to temporal changes in the connectivity of the river network (e.g., Jackson and Leeder, 1994; Gawthorpe and Leeder, 2000; D'Agostino et al., 2001; Connell et al., 2005; Larson et al., 2014; Reheis et al., 2014; Duffy et al., 2015; Repasch et al., 2017; Geurts et al., 2018). Endorheic basins have their own local base level and support permanent or playa lakes depending on the prevailing climatic conditions. Exorheic basins are fluvially connected with adjacent basins in an often predominantly axial (parallel to fault-strike) direction. For
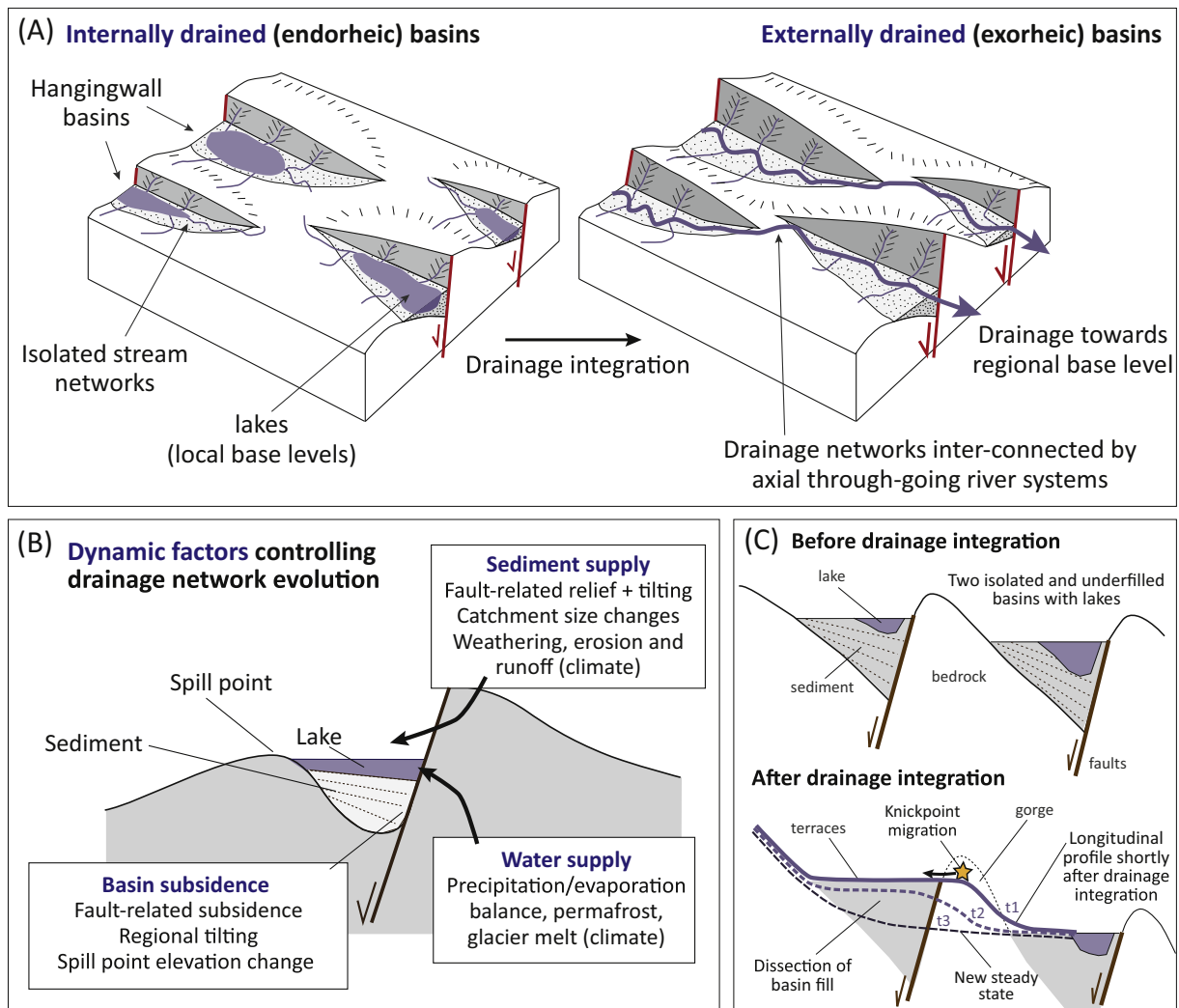
Fig. 1. (A) Long-term drainage integration showing the fluvial integration of initially isolated basins with one another during active extension (schematic). (B) Overview of factors that control sediment supply, water supply and basin subsidence and therefore can change the connectivity of the drainage network by means of overspill mechanisms. We only show 'dynamic factors', which are factors that can produce changes in sediment supply and water supply and the rate of basin subsidence during the time period of active extension. (C) Schematic cross section through two subsiding basins that are initially isolated from one another (top). Overfilling of the upstream basin leads to the integration of both basins by a through-going river system (bottom). The longitudinal profile of this river contains a knickpoint that migrates upstream as the river adjusts to its new boundary conditions (t1, t2, t3 represent different moments in time). This leads to strong incision in the area of the former spill point and in the upstream basin fill, leading the formation of a bedrock gorge and fluvial terraces.

many extensional systems it has been suggested that endorheic drainage predominates during early stages of extension and that these initially isolated basins progressively become integrated over time, either during the period of active extension (Fig. 1A; e.g., Gawthorpe and Leeder, 2000; D'Agostino et al., 2001; Duffy et al., 2015; Gawthorpe et al., 2018), or after extension has largely ceased (e.g., Meek, 1989; Connell et al., 2005; House et al., 2008; Menges, 2008; Phillips, 2008; Larson et al., 2014; Reheis et al., 2014; Repasch et al., 2017). Despite the major importance of drainage network evolution for basin stratigraphy, transient landscape evolution, and the propagation of climatic and tectonic signals across the landscape, our understanding of this process remains limited (e.g., Gawthorpe and Leeder, 2000; Allen and Allen, 2013; Larson et al., 2017; Geurts et al., 2018).

Long-term drainage integration can be partly explained by fault growth and structural linkage of adjacent fault segments that affect the topography of intra-basin areas (e.g., Gawthorpe and Leeder, 2000; Cowie et al., 2006). However, it is increasingly recognised that the lacustrine-fluvial system itself plays an important role in establishing fluvial connections between different basins. One way that the drainage of initially isolated basins becomes integrated is by means of upstream-directed (bottom-up) basin capture by headward eroding rivers (e.g., D'Agostino et al., 2001). Another mechanism is the downstream-directed (top-down) successive overfilling and overspill of basins (e.g., Geurts et al., 2018). The relative importance of these opposing mechanisms of drainage integration, and how they can be

differentiated remains contentious (e.g., Bishop, 1995; Douglass et al., 2009; Larson et al., 2017; Geurts et al., 2018; Meek, 2019). This is partly because the process of headward erosion is not well understood and its efficiency is largely unconstrained (e.g., Douglass et al., 2009). Conclusive evidence for basin overspill, on the other hand, is often poorly preserved because of the intense erosion following drainage integration events. However, in extensional areas for which we have sufficient temporal constraints on basin stratigraphy, the spatio-temporal pattern of drainage integration might allow us to differentiate between them (e.g., Repasch et al., 2017; Geurts et al., 2018).

One extensional area where the connectivity of the drainage network has clearly changed over time is the central part of the Italian Apennines (Fig. 2). Since the Late Pliocene, ca. 3 Ma, this region has been affected by both regional uplift and active extensional deformation, which is accommodated by a ~60 km wide fault array located along the crest of the mountain range (Fig. 2; e.g., Cowie and Roberts, 2001; D'Agostino et al., 2001; Roberts and Michetti, 2004; Faure Walker et al., 2012). The presence of lacustrine sediment in the deeper parts of the basin fills has been used to argue that most basins were endorheic during early stages of extension, but have become fluvially integrated over time (e.g., Cavinato et al., 2000; D'Agostino et al., 2001; Miccadei et al., 2002; Bosi et al., 2003; Piacentini and Miccadei, 2014). Drainage integration has been mainly explained by the active capture of intermontane extensional basins by means of headward erosion from the coast (e.g., D'Agostino et al., 2001).
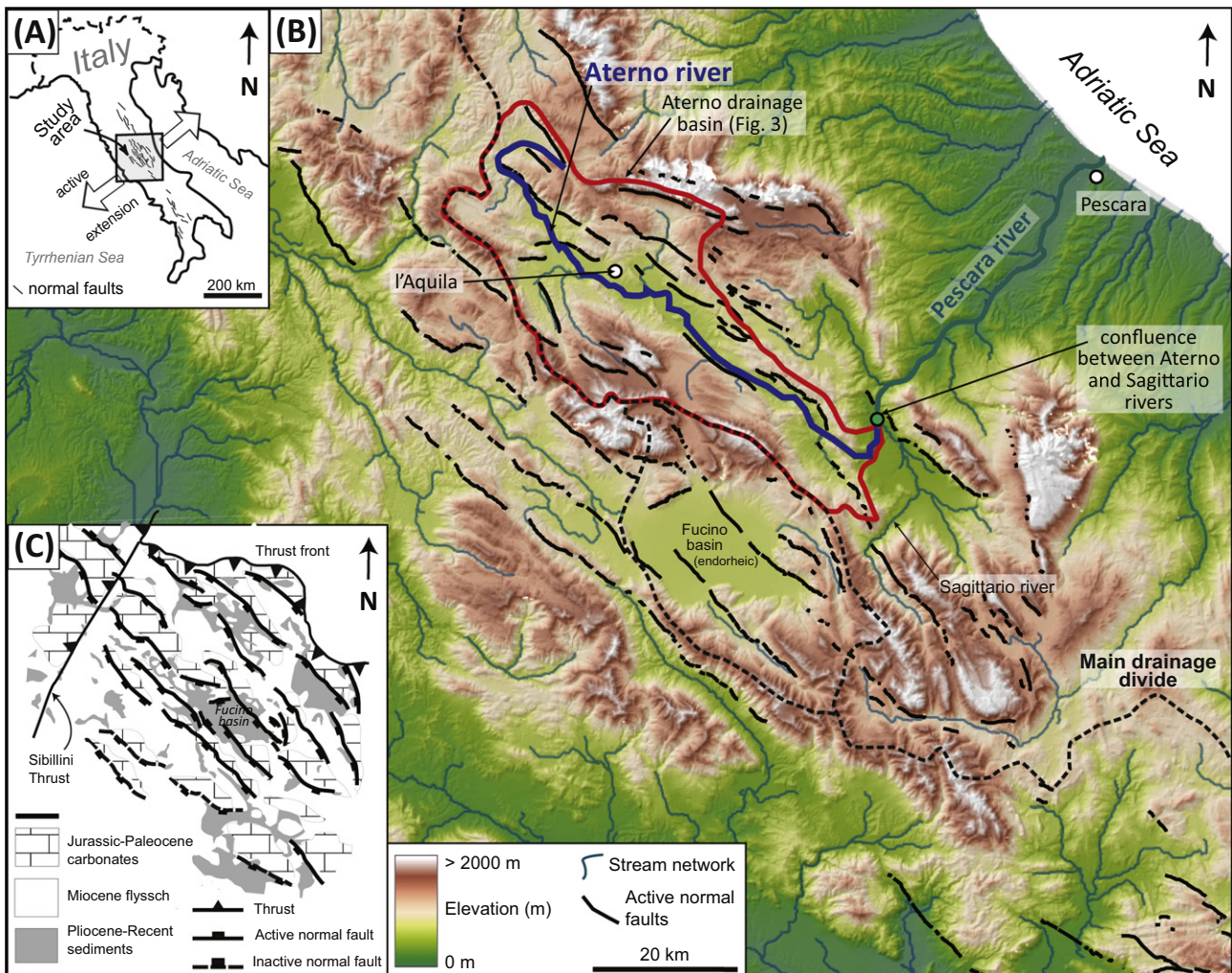
Fig. 2. (A) Location map of the study area in central Italy. (B) Topography of the central Apennines (DEM from Tarquini et al. (2007)) with the drainage network and active normal faults (modified from Roberts and Michetti, 2004). It also shows the catchment of the Aterno River and the large endorheic Fucino basin located at the main drainage divide separating the Tyrrhenian from the Adriatic domain. (C) Simplified geological map of the research area showing the main lithological units (modified from Whittaker et al., 2008).

More recently, numerical modelling work (Geurts et al., 2018) has been used to argue that drainage network evolution in the central Apennines could alternatively be controlled by basin overspill and thus the balance between fault-related basin subsidence and the supply of water and sediment to basins (Fig. 1B). In this model, even when climate is constant, drainage integration results from a long-term increase in sediment supply driven by the increase in footwall topography. The modelling additionally demonstrates how drainage integration leads to deep fluvial incision and terrace formation when the integrated river system geomorphically adjusts to its new base level (Fig. 1C).

The aim of this paper is to use field evidence from the central Italian Apennines to evaluate the predictions of drainage network evolution of Geurts et al. (2018). We focus on the Aterno River system because this area, particularly around the city of L'Aquila, has been the focus of substantial research following the major earthquakes in 2009 (e.g., Giaccio et al., 2012; Mancini et al., 2012; Santo et al., 2014; Pucci et al., 2015; Macri et al., 2016; Porreca et al., 2016; Nocentini et al., 2017, 2018). We integrate published basin stratigraphic data with new geomorphological constraints in order to reconstruct the evolution of the Aterno River system over the last 3 Myr. We use this dataset to evaluate the main factors and mechanisms controlling drainage evolution, and evaluate the impact that drainage network integration has on basin stratigraphy and transient landscape evolution. This is the first time, to our knowledge, that drainage-network-controlled landscape transience has been evaluated in detail for an extensional province that is highly active (regional extension ~3 mm yr^{-1}) and well-understood in terms of fault development (e.g., Roberts and Michetti, 2004; Cowie et al., 2017) and where other factors such as damming of rivers by volcanic activity (e.g., Repasch et al., 2017) have not played any obvious role.

2. Geological setting

The broad morphology of the Italian Apennines results from convergence between the African, Adriatic and Eurasian plates and has led to the formation of a Neogene NE-verging imbricate fold and thrust belt (e.g., Patacca et al., 1990; Royden, 1993). In the central Apennines subduction of oceanic lithosphere ceased by around 6 Ma, and thrust sheets mainly consisting of Mesozoic platform limestone are locally overlain by syn-tectonic Miocene flysch (Fig. 2; Patacca et al., 1990; Montone et al., 2004; Vezzani et al., 2010). Since approximately 3 Ma, the interior part of the central Apennines has been affected by extensional deformation accommodated by a > 60 km wide array of mainly southwest dipping normal faults (Lavecchia et al., 1994; Cowie and Roberts, 2001; Roberts and Michetti, 2004; Fig. 2). Stratigraphy in the hangingwall basins to these normal faults has been dated using palaeontology and tephrochronology and indicate that extension started in what is now the area of the Central Apennines at ca. 3–2.5 Ma (Cosentino et al., 2017).

Contemporaneously with extension, the central Apennines has also undergone >800 m differential uplift relative to the Adriatic and Tyrrhenian coastlines (e.g., D'Agostino et al., 2001; Centamore and Nisio, 2003; Pizzi, 2003; Ascione et al., 2008). The long-term development of this regional topographic 'bulge' that extends >200 km along-strike along the Italian Peninsula is evidenced by marine shorelines perched at least several hundreds of meters above sea level (D'Agostino et al., 2001; Mancini et al., 2007) and shoreface deposits of Early Pleistocene age, fringing the Tyrrhenian and Adriatic flanks of the central Apennines (Pizzi, 2003; Cantalamessa and Di Celma, 2004; Artoni, 2013). Prior to regional uplift, the area was close to sea level allowing marginal marine and brackish sediment to accumulate at the base of some of the extensional basins (Gliozzi and Mazzini, 1998).

Today, much of the area lies at a mean elevation >800 m and elevations in the Apennines reach >2500 m in the footwalls of the largest normal faults. Total throw estimates along the faults vary across the area, but tend to be greatest (up to 2200 m) across the more centrally located, higher elevation fault segments, which have lengths of up to 40 km

(Cowie and Roberts, 2001; Roberts and Michetti, 2004). Geodetic levelling and GPS velocity measurements over a length scale of 100–150 km suggest a regional extension rate of ~3 mm yr^{-1} and an uplift rate of ~1 mm yr^{-1} in the interior part of the central Apennines (D'Anastasio et al., 2006; D'Agostino et al., 2011; Serpelloni et al., 2013; Faccenna et al., 2014). Surface uplift, regional extension rates, topographic elevation, and also the width of the mountain range are all enhanced compared to along-strike adjacent parts of the Apennines, suggesting that the magnitude of uplift and extension are coupled to the same underlying geodynamic mechanism (Faure Walker et al., 2012). While the broad relationship between thrusting and extension in Italy has been argued to be driven by roll-back of what is now the Calabrian Arc (e.g., Magni et al., 2014), it is generally accepted that the magnitude of active surface uplift and extensional faulting over the last ~3 Myr in the Central Apennines must also be the result of dynamic, mantle-driven processes (e.g., Cavinato and DeCelles, 1999; D'Agostino et al., 2001; Faccenna et al., 2014).

The highest Holocene throw rate estimates that exist for faults located in the central Apennines reach up to ~1–2 mm yr^{-1} (e.g., Roberts and Michetti, 2004; Lavecchia et al., 2012; Cowie et al., 2017). These fault throw rates, combined with the measured geological throws would suggest basin initiation ages that would be substantially younger than 3 Ma. Consequently, Roberts and Michetti (2004) argue that faults in the central Apennines had throw rates in the order of 0.3–0.35 mm yr^{-1} during early stages of extension, which then increased for some faults as fault segments evolved, interacted and/or linked. Both structural and geomorphological studies suggest that faults located in the central and highest elevation areas of the array increased their slip rate at ca. 0.8 Ma, whereas faults nearer the edge of the fault array either kept a more-or-less constant slip rate, or became inactive (Cowie and Roberts, 2001; Roberts and Michetti, 2004; Whittaker et al., 2007, 2008). Along some faults, slip rates decreased because of a shift in the locus of activity to neighbouring faults (e.g., Giaccio et al., 2012; Cosentino et al., 2017).

The numerous hangingwall basins in the central Apennines are filled with up to 900 m of continental deposits (e.g., Cavinato et al., 1993; Cavinato and Miccadei, 2000; Cavinato et al., 2002; Miccadei et al., 2002; Nocentini et al., 2017, 2018). The sedimentological characteristics of these deposits are highly variable, comprising fluvial and proximal deltaic sands and conglomerates, distal lacustrine silts and clays, and poorly sorted basin margin deposits originating from debris flows and various types of mass wasting. Most basin stratigraphies, except from the closed Fucino basin (Fig. 2), show a long-term transition from mainly lacustrine to fluvial deposition or fluvial incision, which can be explained by the reorganisation and long-term integration of the drainage network (D'Agostino et al., 2001; Bartolini et al., 2003; Piacentini and Miccadei, 2014; Geurts et al., 2018). Although many basins show this long-term trend, there is considerable variability of stratigraphy and evolution between them that is still largely unexplained (e.g., Bosi et al., 2003; Cosentino et al., 2017).

Various types of palaeoenvironmental records from central Italy in combination with sedimentological and geomorphological observations from the central Apennines demonstrate the impact of Quaternary climatic changes on erosion and sediment transport. Tucker et al. (2011) demonstrate that limestone weathering in the central Apennines occurred >10 times faster during the Last Glacial Maximum (LGM) because of frost cracking and reduced vegetation cover, producing enhanced erosion rates up to 30 times higher than Holocene values. While palynological records and hydrological models suggest precipitation during the LGM was similar to today or even slightly reduced (e.g., Ramrath et al., 1999; Jost et al., 2005; Wu et al., 2007), lake-level reconstructions imply considerably wetter conditions (Giraudi, 1989; Giraudi and Frezzotti, 1997). This discrepancy can be explained by the presence of discontinuous permafrost and glacial meltwaters that increased runoff (Giraudi and Frezzotti, 1997; Bogaart et al., 2003; Kettner and Syvitski, 2008; Tucker et al., 2011). Higher lake levels may
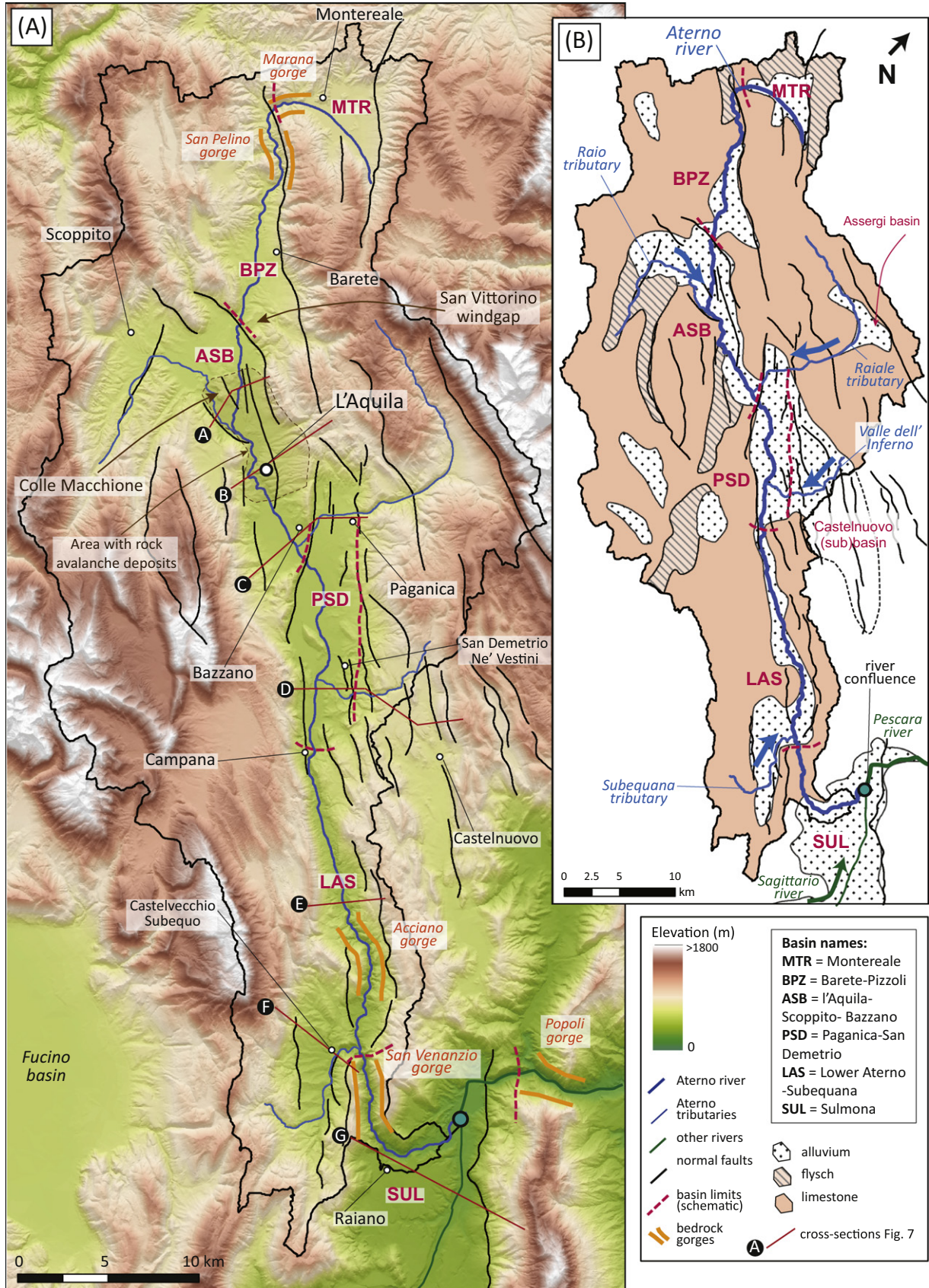
Fig. 3. (A) Topography of the Aterno River catchment, showing the location of the Aterno River that successively crosses the Montereale (MTR), Barete-Pizzoli (BPZ), L'Aquila-Scoppito-Bazzano (ASB), Paganica-San Demetrio (PSD), Lower Aterno-Subequana (LAS), and Sulmona (SUL) basins. It also shows the location of bedrock gorges and the location of the stratigraphic cross sections shown in Fig. 7. (B) Lithology of the Aterno River catchment, the location and geometry of the six major extensional basins, and the main tributaries of the Aterno River.

have also resulted from a higher precipitation/evaporation ratio during cold glacial conditions. Enhanced discharge for mountain streams is also supported by the coarser calibre of clasts observed in fluvial conglomerates formed during glacial times (Whittaker et al., 2010; Whittaker and Boulton, 2012).

3. Data and methodology

Our approach is to integrate geomorphological and stratigraphic data for the present-day Aterno River system (Figs. 2 and 3). Our focus is to identify changes to the drainage pattern of this river system over the last 3 Myr, in particular drainage integration and isolation events, which influenced the connectivity between the different basins along the Aterno River. We assume the locations of the main valleys and hangingwall depocentres of the Aterno River system were established during the early stages of extension and have remained largely unchanged since then. We base this assumption on the observation that the boundary of the Aterno drainage network today is confined by high topography, by the pattern of active normal faulting (Roberts and Michetti, 2004; Nocentini et al., 2017, 2018) and by the structures inherited from the earlier phase of compressional tectonics (e.g., Piacentini and Miccadei, 2014; Geurts et al., 2018); these structures equally limit the spatial extent of Early to Middle Pleistocene hangingwall lacustrine sediment. Only in the Castelnuovo sub-basin (see below and Fig. 3), is there evidence that a valley formerly linked with the Aterno system now drains elsewhere. Consequently, as we discuss in detail in the results, the Aterno River system today spatially integrates these previously endorheic sub-basins via low elevation 'spill-points' that lie between them.

3.1. River profile and terrace analysis

We used the longitudinal profile of the Aterno River to assess whether the river system is undergoing a transient erosional response to drainage integration over time. We extracted this from a 10 m DEM of central Italy (Tarquini et al., 2007) and manually identified marked concave reaches and knickzones (i.e., over-steepened or convex reaches). For all knickzones we evaluated whether they could be explained by lithological contrasts using detailed geological maps of the area (e.g., Vezzani and Ghisetti, 1998). For lithological contacts between flysch and limestone in the western part of the central Apennines, Whittaker et al. (2008) estimated a maximum convexity height of ~100 m upstream of these boundaries for small streams with a drainage area of ~10 km^2. Even though the lithological contrasts in our study area mainly comprise limestone-alluvium alternations, the 10 to 100 times larger drainage area of the Aterno River is expected to strongly limit the heights of lithology-related knickzones as a higher discharge increases stream erosivity (Stock and Montgomery, 1999).

We also evaluated whether the knickzones along the Aterno River could be explained by a transient response to fault slip acceleration. For fault block-scale catchments in the western part of the central Apennines, Whittaker et al. (2007, 2008) demonstrated how streams had steepened and narrowed their channel directly upstream of faults that had been documented to have increased their slip rate ca. 0.8 Ma. Based on the position of knickzones relative to the pattern of active normal faults that are mapped for the Aterno River catchment (Roberts and Michetti, 2004; Nocentini et al., 2017, 2018), we therefore evaluated whether any knickzones could be explained by an increase in slip rate on these faults since their initiation (Cowie and Roberts, 2001).

For knickzones for which a lithological and/or fault-related origin could be excluded, we evaluated whether they could be produced by drainage integration events, i.e., two different river profiles becoming one. First we looked for transitions from lacustrine to fluvial sedimentary facies in the basin located upstream of the knickzone, something we explain in more detail below (in Section 3.2). In the case of a drainage integration event, the transition from endorheic to exorheic

conditions in the upstream basin is expected to lead to river incision and the formation of a depositional terrace that primarily consists of endorheic (often lacustrine) sediment (e.g., Garcia-Castellanos et al., 2003; Connell et al., 2005; House et al., 2008; Menges, 2008; Larson et al., 2017; Repasch et al., 2017). Therefore we analysed the character of the main depositional terraces in each basin using geological maps, cross sections and the DEM of the area (Miccadei et al., 2002; Bosi et al., 2004; Chiarini et al., 2014; Piacentini and Miccadei, 2014; Nocentini et al., 2017, 2018) and estimated their top elevation. When estimating the elevation of the individual terraces, we attempted to use only terrace remnants whose elevation relative to the Aterno River was not expected to be significantly affected by active faulting (see Supplementary Materials A for details).

3.2. Basin stratigraphy

We compiled and compared the infilling histories of six major fault-controlled basins to reconstruct the development of the Aterno River system, and synthesised published stratigraphic data from these basins into one integrated stratigraphic scheme. These basins comprise the Montereale basin (MTR), the Barete-Pizzoli basin (BPZ), the L'Aquila-Scoppito-Bazzano basin (ASB), the Paganica-San Demetrio basin (PSD), the Lower Aterno-Subequana basin (LAS), and the Sulmona basin (SUL; Fig. 3). The data come from numerous detailed studies of individual basins (Miccadei et al., 2002; Bosi et al., 2004; Chiarini et al., 2014; Pucci et al., 2015; Gori et al., 2017; Nocentini et al., 2017, 2018) but also from some studies that compared several basins from the central Apennines with one another (e.g., Bosi et al., 2003). To evaluate the impact of extensional faulting on basin geometry, we additionally compiled data on the total sediment thickness from seismic and borehole studies (Miccadei et al., 2002; Santo et al., 2014; Chiarini et al., 2014; Gori et al., 2017).

We identified in each basin's stratigraphic record units that likely formed when basins were underfilled – indicated by the widespread presence of lacustrine (or palustrine) sediment. We used these units to identify when the basin likely did not have any fluvial outlet (i.e., endorheic drainage). In contrast we assumed the presence of fluvial stratigraphy to reflect phases in a basin's evolution when overfilled and exorheic conditions occurred, i.e., when basins were fluvially connected with their downstream neighbour or with the Adriatic coast. In the central Apennines, lacustrine deposits comprise a number of different facies. Most important for our identification of underfilled conditions were deep lake deposits that generally comprise white-grey, laminated to massive calcareous clays and silts with occasional intervening layers of sand or gravel (e.g., Miccadei et al., 2002; Gori et al., 2017; Nocentini et al., 2017, 2018). The input of coarser clastic material typically becomes more abundant towards the basin margins where the deep-water facies pass laterally into either delta, alluvial fan or slope deposits. To estimate the timing of these transitions we used age estimates from lacustrine or fluvial units that encompass the transition most precisely. These age estimates are provided by published palaeomagnetic, biostratigraphic and tephra analyses, the latter comprising both lithotype analysis and radioisotope dating (e.g., Galli et al., 2010; Magri et al., 2010; Palombo et al., 2010; Giaccio et al., 2012; Mancini et al., 2012; Chiarini et al., 2014; Gori et al., 2015, 2017; Nocentini et al., 2017, 2018).

In addition, we examined vertical facies successions to provide insight into changes in the balance between sediment supply and basin subsidence (in volumetric terms) and to identify major shifts in depositional environment associated with abrupt lacustrine deepening, shallowing, or with fluvial incision. Most important were shallowing-upward stratigraphic motifs, for instance deep lake facies passing gradually upward into prograding delta deposits, which suggest a change from under- to overfilled conditions. We also integrated information on the sedimentary contact between lacustrine and fluvial units, for instance whether it is an erosional unconformity or a gradual transition. Furthermore, we made a compilation of the stratigraphic cross sections

that are available for the four southernmost basins, i.e., the ASB, PSD, LAS and SUL basins, as these provide insight into the stratigraphic position of the different units relative to one another, their geometry, and potential shifts in fault activity over time. These published cross sections are primarily based on well logs, and in some cases, additionally on seismic profiles (Miccadei et al., 2002; Piacentini and Miccadei, 2014; Nocentini et al., 2017, 2018). We used the amount of relief of the top surface of the endorheic basin fill to estimate the amount of incision that followed drainage integration events. The final preserved thicknesses (without decompaction) and ages of the lacustrine units were also used to estimate long-term sedimentation rates. Given that part of these lacustrine records may have been eroded as a consequence of drainage integration events, these sedimentation rates are minimum estimates.

In general, we focus on the stratigraphic and geomorphological observations that are most closely related to the development of the Aterno River, however, many observations come from incised terraces along the basin margins. Even though this generates uncertainties, we believe the available data from the Aterno River catchment is sufficient to allow us to reconstruct the development of the axial parts of the basins to first order. This approach also explains the way we analysed the Paganica-San Demetrio (PSD) basin that is commonly considered as a sub-basin of the much larger Paganica-San Demetrio-Castelnuovo basin (Fig. 3B). We focused mainly on the PSD sub-basin as it has recorded not only the Early (to early Middle) Pleistocene lake that covered both the PSD and Castelnuovo sub-basins, but also the successive development of the Aterno River.

4. The Aterno River system and associated rift basins

The Aterno River is the largest river system draining the Adriatic domain of the central Apennines (Figs. 2 and 3). It has a length of ~100 km, a drainage area of ~1300 km^2, and flows axially over most of its length (i.e., approximately parallel to fault strike). Within its catchment, elevations vary between ~2500 and 250 m above sea level. Even though the river is perennial and has continuous flow throughout most years, it is characterised by a highly variable, seasonal discharge regime with a modern-day minimum, mean and maximum discharge of ~0.08, 5.2 and 143 m^3/s within its downstream reach, near its entrance to the San Venanzio gorge (Lastoria et al., 2008; Fig. 3A).

The headwaters of the present-day Aterno River are located in the uplands surrounding the Montereale (MTR) basin (Fig. 3). The river first flows across the MTR basin (at ~820 m elevation) and through the Marana gorge in a southwest (across-strike) direction for ~10 km. Downstream of the MTR basin the river starts flowing in a predominantly southeast (along-strike) direction over a distance of ~85 km, across successively the Barete-Pizzoli (BPZ), L'Aquila-Scoppito-Bazzano (ASB), Paganica-San Demetrio (PSD), and Lower Aterno-Subequana (LAS) basins. Downstream of the LAS basin the river flows through the San Venanzio gorge and continues across the Sulmona (SUL) basin where it turns to the northeast (across-strike) and meets with the Sagittario River at ~250 m elevation. From here the combined Aterno-Sagittario River continues in a northeast direction through the Popoli gorge and into the Adriatic foreland area where it is called the Pescara River (Fig. 3).

4.1. River profile and terrace analysis

Fig. 4A shows the DEM-derived longitudinal profile of the Aterno River as well as its downstream continuation as the Pescara River towards the Adriatic coast. The longitudinal profile reveals three large, convex-up knickzones (each >100 m high), which have been ground-truthed by field surveys (yellow in Fig. 4B). The most prominent knickzone lies directly upstream of the SUL basin, at ~250 m, where the Aterno River flows through the San Venanzio bedrock gorge from the LAS basin. This knickzone extends approximately 30–35 km

upstream, to an elevation of ~550–575 m (Fig. 4A and B). In detail, this convex reach itself comprises a number of small-scale convexities, which can be partly attributed to alternations between limestone bedrock and alluvium, e.g., around the Acciano bedrock gorge (Fig. 4A and C).

A second, large convex reach with a height and length of ~100 m and 10 km, respectively, is located in between the two most upstream basins, the MTR and BPZ basins (Fig. 4A and B). Along this reach the Aterno River crosses both the active Monte Marine Fault (also known as Barete Fault; Roberts and Michetti, 2004) and the Marana and San Pelino bedrock gorges, located in the footwall and hangingwall of the Monte Marine Fault, respectively (Fig. 4A and B). Between these two major convex reaches, the overall shape of the Aterno longitudinal profile is concave, except for a number of knickpoints smaller than 30 m (Fig. 4A and B). Along the Pescara River, i.e., in between the downstream end of the Aterno River and the Adriatic coast, the longitudinal profile exhibits another convexity that is ~15 km long and 150 m high between the SUL basin and the foreland area (Fig. 4A and B). Here the river crosses the Popoli gorge and the tip of the Monte Morone Fault (also referred to as the Sulmona Fault; Roberts and Michetti, 2004).

Along much of its course, the modern-day Aterno River has an incised position within the youngest parts of the basin fills (Fig. 4A). Either depositional or erosional terraces with top elevations <10–20 m above the Aterno thalweg have been described for the ASB, PSD, and SUL basins and are interpreted to be a product of the last glacial-interglacial cycle (Miccadei et al., 2002; Nocentini et al., 2017, 2018). However, in many basins we also observe at least one significantly higher depositional surface that forms the upper limit of the basin fill and has elevations that vary in between 30 and 150 m above the Aterno River (Fig. 4A). The most prominent of these depositional surfaces, varying between ~550 and 600 m elevation, are within the LAS basin (Figs. 4A and 5A; e.g., Gori et al., 2017), and the extensive 'Terrazza Alta di Sulmona' at ~350–400 m elevation in the SUL basin (e.g., Miccadei et al., 2002). It is important to note that the age and sedimentological characteristics of these prominent terraces vary among the different basins (Fig. 4A; see Supplementary Materials A for details). However, what they have in common is that they may all relate to the integration of the drainage network, and we develop this idea further below.

4.2. Basin stratigraphy

The total thickness of syn-rift sediments varies considerably along the Aterno River from zero within the bedrock limestone reaches to >400 m within the deepest hangingwall basins (grey shading, Fig. 4A). This spatial variability can be largely explained by the pattern of extensional faulting. Within individual basins, there is significant variability in sediment thickness, as for instance within the ASB, PSD, and LAS basins. This intra-basin variability can primarily be explained by the fact that many of these large basins are controlled by multiple faults. Moreover, in some basins, transverse faults (i.e., striking approximately SW-NE) additionally affect basin geometry and hence the pattern and rates of basin subsidence (e.g., Santo et al., 2014; Gori et al., 2017).

Fig. 6 summarises the stratigraphy for each basin along the Aterno River, and Fig. 7 shows stratigraphic cross sections through the four southernmost basins. For most basins the onset of infilling is poorly constrained to the beginning of the Early Pleistocene based on the regional onset of extensional faulting in this area (D'Agostino et al., 2001; Cosentino et al., 2017). In case of the PSD and ASB basins, however, biostratigraphic dating suggest that sedimentation started at, or before, the Pliocene-Pleistocene transition (Cosentino et al., 2017; Fig. 6). In this section we describe the most important aspects of the individual basin stratigraphies that provide insights into when and where endorheic or exorheic conditions existed, and how transitions between them might have occurred. We mostly adopt lithofacies names instead of local formation names in order to increase the readability of the
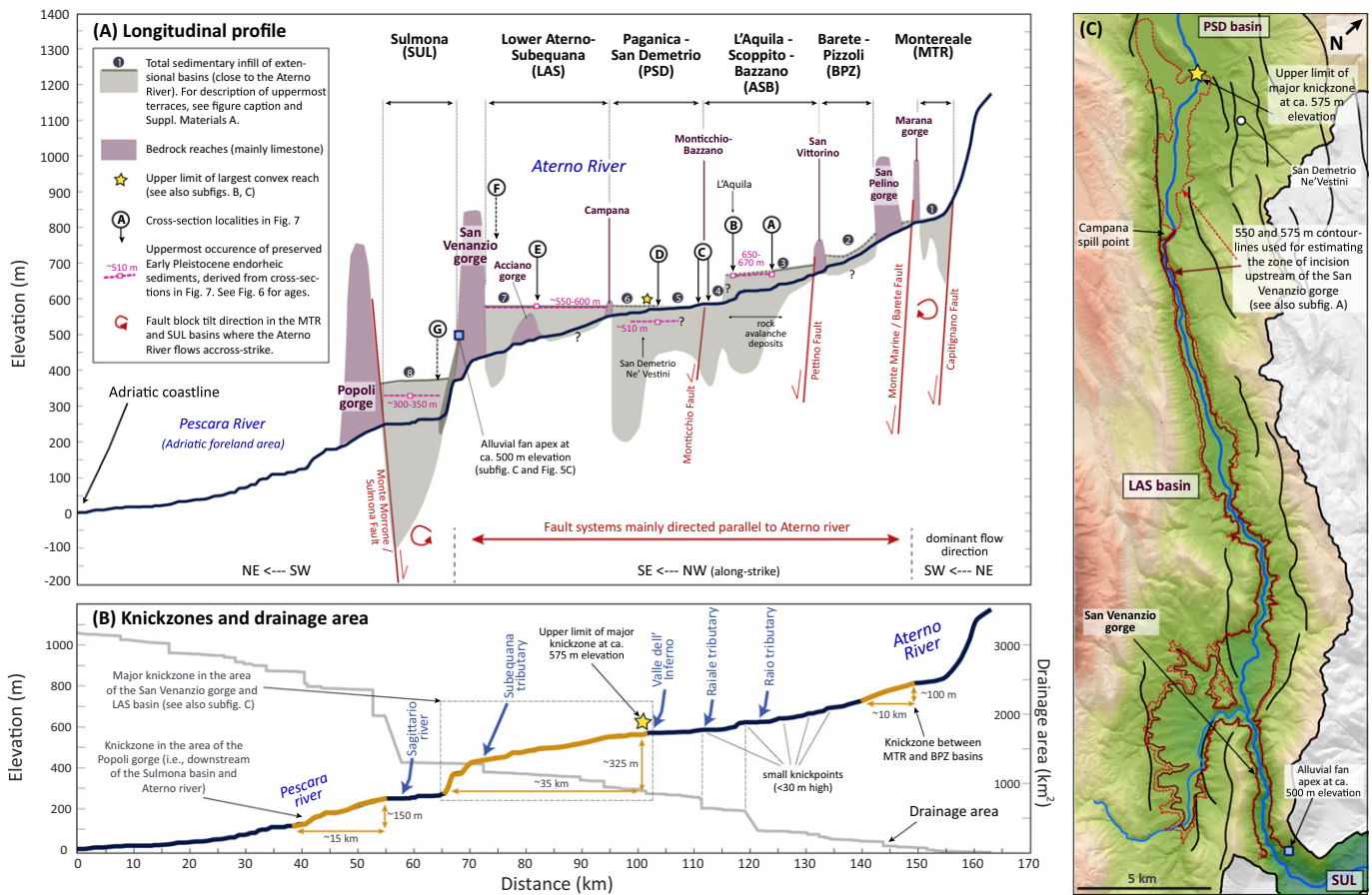
Fig. 4. (A) Longitudinal profile of the Aterno River, the location of the different extensional basins, and their (bedrock) spill point areas. Most basin-bounding fault systems are orientated parallel to the river and are therefore not shown individually. We do show, however, the position of those fault systems with strike approximately perpendicular to the river. Pink squares and pink dashed lines show the approximate elevation of the sedimentary contact between the endorheic (lacustrine/palustrine/deltaic) and exorheic (fluvial) sediment in the four southernmost basins, based on the cross sections shown Fig. 7. Also shown are the approximate upper- and lowermost elevation of the basin sedimentary fills. The upper elevations are based on the top elevation of the uppermost terraces (dark grey lines) that we selected along the river. We selected terraces consisting of fluvial or lacustrine sediment and excluded those consisting of rock avalanche / debris flow deposits in the Colle Macchione-L'Aquila area (see Supplementary Materials A for details): (1) Main (active) fluvial plain of the MTR basin at ~815 m elevation, (2) Early Pleistocene (age poorly constrained) terraces consisting of fluvial and lacustrine sediment. The elevation of its top surface varies considerably across the basin, likely because of differential basin subsidence. (3) Terraces with top elevations of ~650–670 m, consisting of late Middle Pleistocene (~MIS5a) fluvial gravel deposits belonging to the 'Fosso Vetoio Synthem' according to Nocentini et al. (2017). (4) Main (active) fluvial plain in the Bazzano sub-basin at ~590 m elevation. Large elevation difference (>50 m) between uppermost terraces between the areas up- and downstream of L'Aquila can be explained by the temporal blocking of the river valley by >50 m thick rock avalanche deposits during the Middle Pleistocene. (5) Main (active) fluvial plain at ~575 m elevation in the PSD basin, upstream of San Demetrio Ne' Vestini. (6) Fluvial terrace morphology borders the Aterno River on both sides in the PSD basin downstream of San Demetrio Ne' Vestini. However, it is uncertain to what extent these terraces are related to fault activity. Based on the longitudinal profile we expect the wave of incision related to the formation of the San Venanzio gorge to have reached the downstream part of the PSD basin and to explain 25 m high terrace morphology in this area. (7) Terraces consisting of Early Pleistocene lacustrine and fluvial deposits with top elevations at ~550–600 m elevation close to the Aterno River. (8) 'Terrazza Alta di Sulmona' at ~350–400 m elevation consisting primarily of >50 m of fluvial gravel, in turn overlying Early to early Middle Pleistocene lacustrine sediment (Miccadei et al., 2002). (B) Large convex reaches (yellow), smaller convexities, tributary confluences, and drainage area accumulation along the Aterno longitudinal profile. (C) Topography of the area of the major knickzone upstream of the San Venanzio gorge. Based on the longitudinal profile of the Aterno River, we expect that the upper limit of this transient knickzone is located at approximately 575 m elevation, i.e., close to San Demetrio Ne' Vestini in the PSD basin (Fig. 4A). However, another option is that the upper limit is located at approximately 550 m, near Campana, i.e., approximately at the border between the PSD and LAS basins. Therefore, we show both the 550 and 575 m contour lines to illustrate the approximate area of fluvial incision caused by knickpoint propagation.

paper, and partly because there is no general agreement on the formation names.

4.2.1. Predominant lacustrine sedimentation during the Early to early Middle Pleistocene

In all basins the Early to early Middle Pleistocene stratigraphy consists at least partly of lacustrine sediment (Figs. 6 and 7). In the most upstream MTR basin, Early to early Middle Pleistocene lake sediments have been observed in its north-eastern sub-basin (Fig. 6; Chiarini et al., 2014). Early Pleistocene lake sediments have also been documented for the adjacent basin, the BPZ basin (Bosi et al., 2004; Piacentini and Miccadei, 2014), however, its spatial extent and age is poorly constrained. In all the other basins farther downstream, i.e., the

ASB, PSD, LAS and SUL basins, lake sediments are widespread and suggest that lakes covered most of their individual hangingwall basins for some periods during the last 3 Myr (Miccadei et al., 2002; Giaccio et al., 2012; Gori et al., 2017; Figs. 6 and 7). In the ASB basin, the area around L'Aquila and Bazzano experienced continued lacustrine sedimentation during the Early Pleistocene, whereas the Scoppito area experienced a transition from an alluvial fan-dominated environment to lacustrine sedimentation around 2–1.7 Ma (Fig. 6; Mancini et al., 2012; Nocentini et al., 2017). These differences in stratigraphy can be explained by a former geomorphological threshold that might have existed half-way down the ASB basin in the area of Colle Macchione (Fig. 3A; Mancini et al., 2012). The lake in the PSD basin was a major lake that also covered the adjacent Castelnuovo basin (cross section D
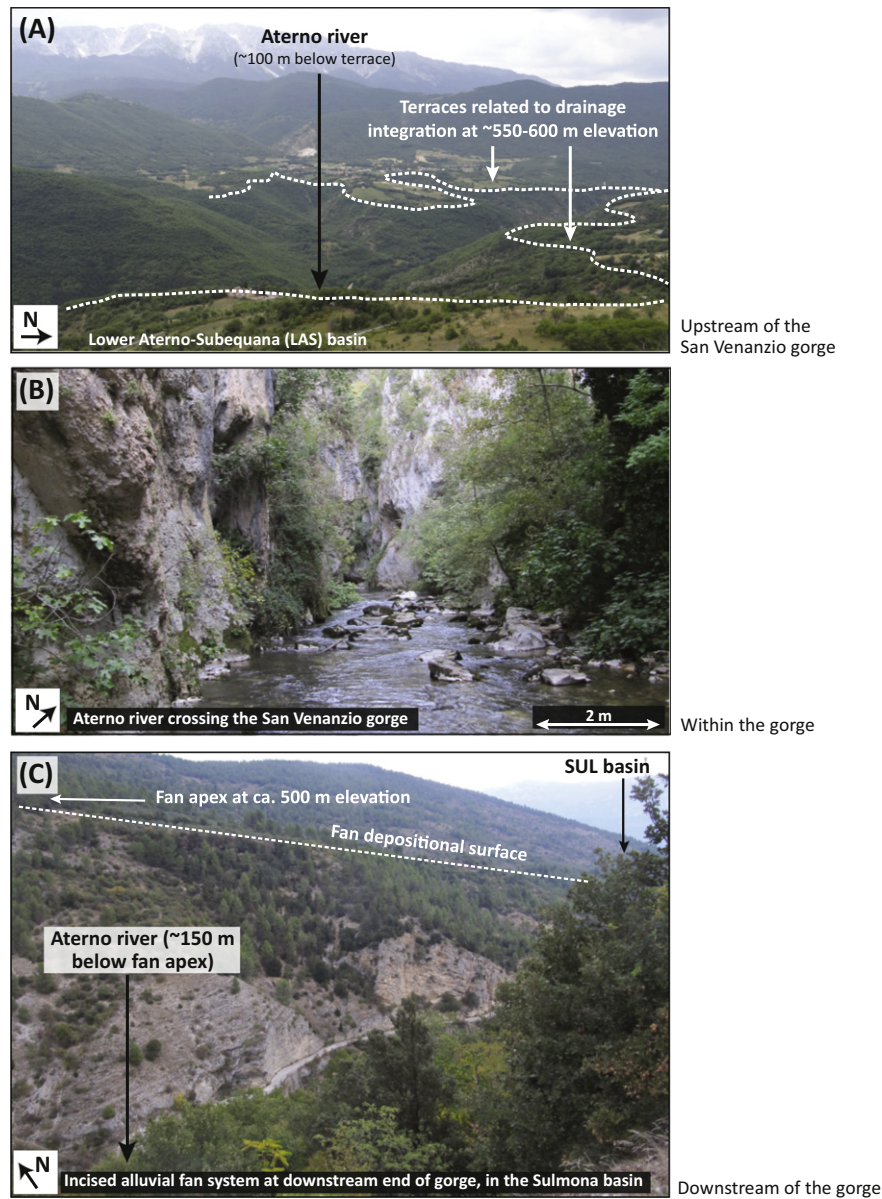
Fig. 5. Pictures taken upstream (A), within (B) and downstream (C) of the San Venanzio gorge. (A) Depositional terraces along the Aterno River in the LAS basin that were formed as a consequence of drainage integration between the LAS and SUL basins. These terraces largely consist of lacustrine sediment with fluvial gravels on top, suggesting the basin to have become overfilled. Overspill towards the SUL basin (ca. 0.7 Ma) led to the formation of a through-going river system that started to incise sediment in the LAS basin and to transport sediment towards the SUL basin, where it initially formed a large alluvial fan system where the downstream end of today's San Venanzio gorge is located (shown in C). On-going incision by the Aterno River led to the progressive dissection of the alluvial fan deposits (in C) and the LAS basin fill (in A) and the formation of the San Venanzio gorge (in B).

in Fig. 7; Giaccio et al., 2012). Water depths in this lake were of the order of 30 m as suggested by the height of Gilbert delta foresets (Giaccio et al., 2012).
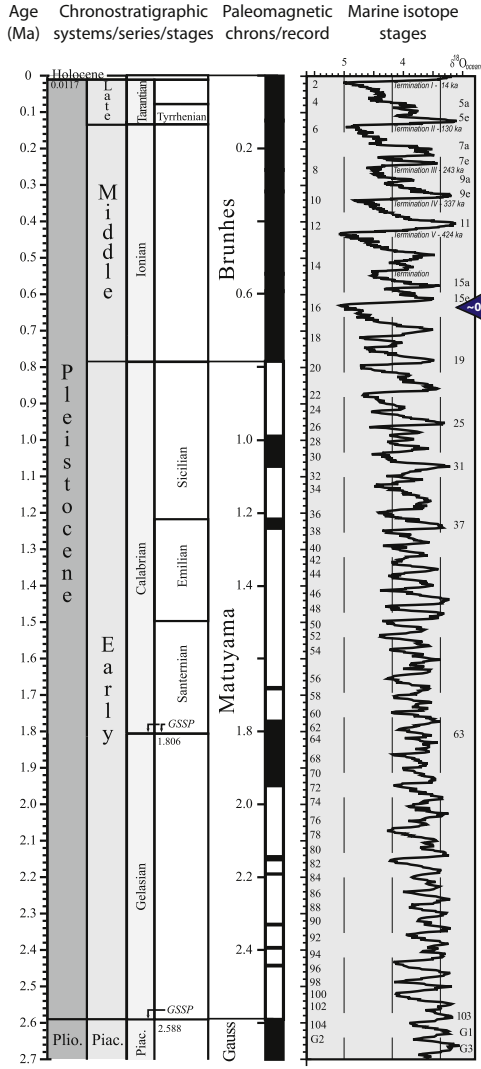
No direct constraints on lake depths exist for the other basins. However, the absence of frequent alternations between shallow and deep lake facies suggests most Early to early Middle Pleistocene lakes to have been sufficiently deep to impede glacial-interglacial climate-related oscillations in lake level (e.g., Giraudi and Frezzotti, 1997) from markedly affecting the sedimentary environment. An exception is the Scoppito part of the ASB basin where the characteristic 'Madonna della Strada' deposits are found between ca. 2–1.7 and 1.2–1.1 Ma (Fig. 6 and cross sections A, B in Fig. 7). These comprise alternating layers of fine (sandy silts and clays) and sandy gravels, with thick lignite seams up to several meters thick (Mancini et al., 2012; Nocentini et al., 2017). Some of these lignites have been correlated to Early Pleistocene interglacial periods (e.g., Magri et al., 2010) and likely formed in

relatively shallow lake or lake margin environments (Mancini et al., 2012; Nocentini et al., 2017).

4.2.2. Transition from endorheic to exorheic conditions during the late Early and early Middle Pleistocene

Our data compilation suggests that either the ASB or BPZ basin was the first to become externally drained. In the ASB basin, lacustrine sedimentation is abruptly followed by fluvial incision (Fig. 6; Mancini et al., 2012; Macri et al., 2016; Porreca et al., 2016; Nocentini et al., 2017). Here, biostratigraphic data from the youngest preserved lacustrine sediment suggests this abrupt change to have occurred around 1.1–1.2 Ma (Mancini et al., 2012; Nocentini et al., 2017). In the BPZ basin, located directly upstream of the ASB basin, lacustrine sediment in the southern part of the basin is covered by fluvial terrace gravels with a reversed magnetic polarity (Figs. 3A and 6; Bosi et al., 2004; Piacentini and Miccadei, 2014). The fact that this fluvial terrace extends into a windgap

Quaternary chronostratigraphy

BASINS:

-SUL- Sulmona | -LAS- Lower Aterno-Subequana | -PSD- Paganica-San Demetrio | -ASB- L'Aquila-Scoppito-Bazzano | -BPZ- Barete-Pizzoli | -MTR- Montereale

Age (Ma) | Chronostratigraphic systems/series/stages | Paleomagnetic chrons/record | Marine isotope stages

Modified from Cohen and Gibbard (2010)

Miccadei et al. 2002
Giaccio et al. 2009, 2013
Zanchetta et al. 2017

Gori et al. 2017
Piacentini and
Miccadei 2014

Giaccio et al. 2012
Pucci et al. 2015
Nocentini et al. 2018

Mancini et al. 2012
Macri et al. 2016
Nocentini et al. 2017

Bosi et al. 2004
Piacentini and
Miccadei 2014

Chiarini et al. 2014

G | E, F | C, D | A, B, C | Cross-sections in Fig. 7
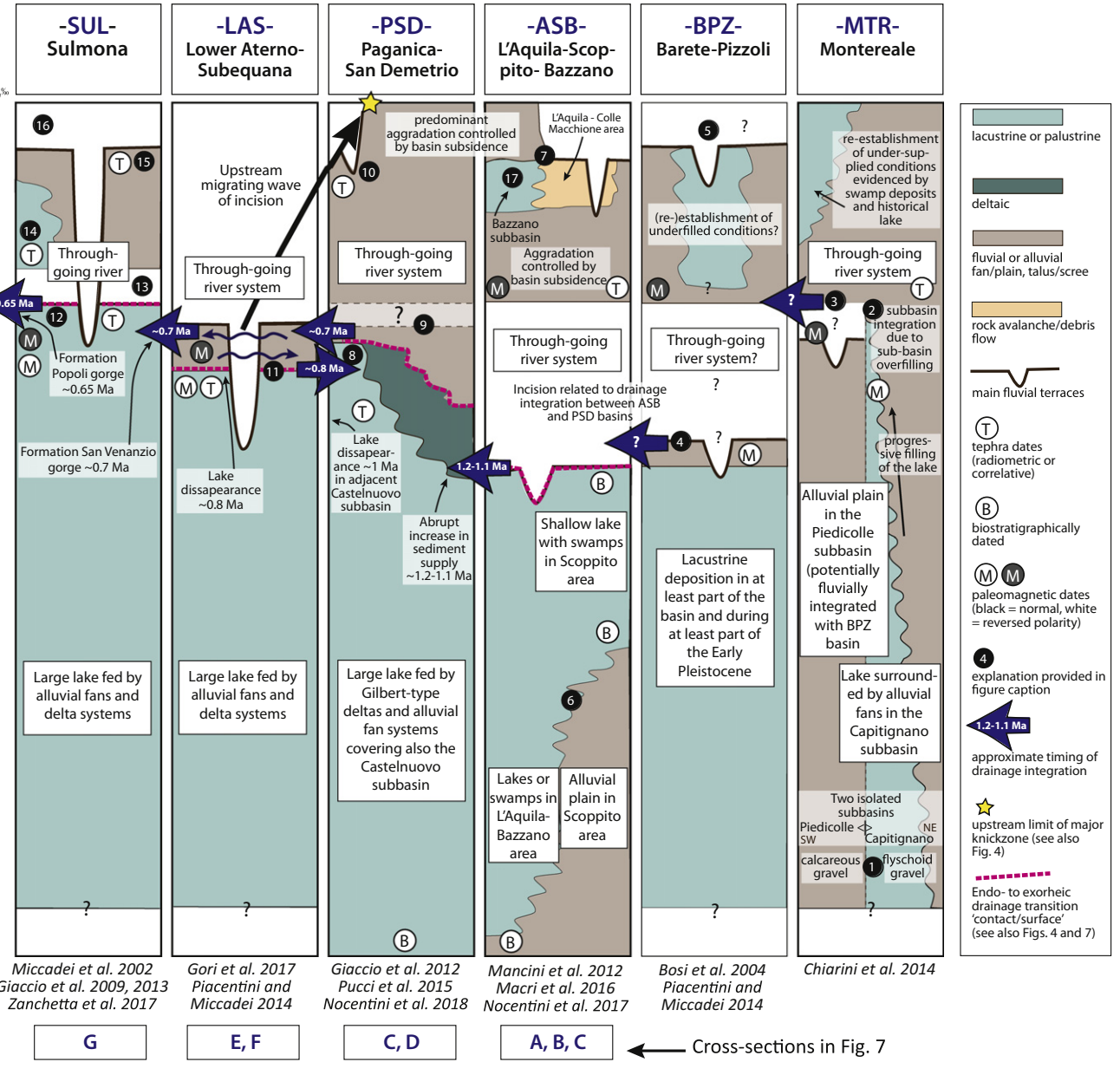
east of San Vittorino (Fig. 3A; also discussed by D'Agostino et al., 2001) suggests that a fluvial connection between the BPZ and ASB basins had been established by the latest part of the Early Pleistocene (Fig. 6).

The LAS basin was likely the third basin to become externally drained between 0.8 and 0.7 Ma (Fig. 6). This integration event is constrained by two $^{40}Ar/^{39}Ar$ dated tephra layers near the top of the lacustrine silts (890 and 805 ka) and a normal magnetic polarity of overlying fluvial gravels (Gori et al., 2015, 2017). In the LAS basin a gradual transition from lacustrine silts into fluvial sands and gravels has been interpreted by Gori et al. (2017) as the basin shallowing and becoming overfilled (Fig. 6 and cross sections E and F in Fig. 7). These oldest fluvial gravels show a flow direction to the northwest, i.e., towards the PSD basin, opposite to the regional flow of the Aterno River (Fig. 3A; Gori et al., 2015, 2017). Thus from at least ca. 1.1–1.2 Ma until ca. 0.8–0.7 Ma, we argue that the PSD basin acted as a local base level, first for the ASB and BPZ basins, and later on, also for the LAS basin. The Castelnuovo basin, which lies parallel, but East of the PSD and LAS basins, started draining towards the PSD basin from ca. 1 Ma onwards (Fig. 3B; Giaccio et al., 2012). In the LAS basin, basin infilling and the establishment of a NW-flowing river was soon followed by deep fluvial incision that is explained by the cutting of the San Venanzio gorge (Gori et al., 2017; Fig. 6 and cross sections E and F in Fig. 7).

In the PSD basin a strong increase in sediment supply from the north occurred around 1.2–1.1 Ma, causing rapid infilling of the lake by large (up to 30 m high) Gilbert-type deltas that are overlain by braided river deposits (Giaccio et al., 2012; Nocentini et al., 2018; Fig. 6 and cross sections C and D in Fig. 7). The formation of the San Venanzio gorge around ca. 0.7 Ma (Gori et al., 2015, 2017) terminated endorheic drainage in the combined BPZ-ASB-PSD-Castelnuovo-LAS area and led to the establishment of a through-going river system all the way towards the southernmost SUL basin. The transition from aggradation to a phase of non-deposition or limited fluvial incision in the PSD basin around ca. 0.8–0.7 Ma (Giaccio et al., 2012), suggests that by that time sediment was largely exported out of the basin by the Aterno River flowing through the San Venanzio gorge (Fig. 6). A large Pleistocene alluvial fan system in the SUL basin at the downstream end of the gorge has been documented, which was likely formed when large quantities of sediment were transported across the former spill-point between the two basins (Figs. 5C, 4A and C; Miccadei et al., 2002; Gori et al., 2015, 2017).

In the SUL basin, lacustrine conditions persisted the longest, until ca. 650 ka, based on radiometric age estimates from multiple tephra layers (Fig. 6 and cross section G in Fig. 7; Giaccio et al., 2013; Zanchetta et al., 2017). Here the lacustrine phase was followed by a period of localised deep (~50 m) fluvial incision, with soil development on the surrounding abandoned terrace surfaces (Zanchetta et al., 2017). This erosion phase is interpreted to have resulted from the opening and incision of the

Popoli gorge and lasted until ca. 530 ka (Fig. 3A; Miccadei et al., 2002; Giaccio et al., 2009, 2013; Zanchetta et al., 2017).

The evolution of the MTR basin is the hardest to connect to the other basins. Here external drainage began somewhere during the Middle Pleistocene, as evidenced by palaeomagnetic analysis of lacustrine sediments (Fig. 6) and the abundance of Middle Pleistocene tephra in the oldest fluvial deposits topping the lacustrine deposits (Chiarini et al., 2014). In case of the MTR basin, an erosional unconformity marks the abrupt transition from lacustrine sedimentation to prograding alluvial fan systems that caused the overfilling of the northeastern sub-basin and its integration with the southwestern sub-basin (Chiarini et al., 2014).

4.2.3. Late Early Pleistocene to Holocene development of the Aterno River

The late Early Pleistocene to Holocene sections of most of the basin stratigraphies either comprise fluvial sediment, or erosion and terrace formation associated with fluvial incision by the Aterno River (Fig. 6). Borehole data from the most upstream located MTR basin suggest that fluvial incision of at least 40 m followed drainage integration with the downstream BPZ basin sometime during the late Early Pleistocene or early Middle Pleistocene (Chiarini et al., 2014). However, the timing of drainage integration as well as the duration of the period of incision in the MTR basin is poorly constrained (Fig. 6). In this basin, aggradation has replaced incision and sediment now fully covers the older erosional terrace morphology.

It is uncertain how much fluvial incision occurred in the BPZ basin directly following drainage integration at the end of the Early Pleistocene. However, the basin primarily experienced aggradation during the Middle Pleistocene as sediment with a normal magnetic polarity partly covers Early Pleistocene terraces. This Middle Pleistocene sediment not only consists of fluvial sand and gravel, but also partly of lacustrine silt and clay (Bosi et al., 2004; Fig. 6). In the central part of the basin, the active floodplains of the Aterno River are incised 15–20 m into these Middle Pleistocene deposits suggesting renewed fluvial incision to have started sometime during the Late Pleistocene. Maximum Holocene throw rate estimates for the main basin-bounding fault system, i.e., the Monte Marine/Barete Fault, vary between ~0.55 and 1 mm yr^{-1} (Roberts and Michetti, 2004; Galli et al., 2011), suggesting that this fault system has accelerated its slip rate over time (see Section 2).

In the ASB basin, drainage integration with the PSD basin around 1.2 Ma was directly followed by fluvial incision of the order of 50–100 m (Mancini et al., 2012; Nocentini et al., 2017; cross sections A, B, and C in Fig. 7). Aggradation started again during the early Middle Pleistocene, causing most of the Early Pleistocene lacustrine sediment to become largely covered by Middle Pleistocene fluvial deposits (Nocentini et al., 2017). During the late Middle Pleistocene, the ASB basin

Fig. 6. Main stratigraphic units for each basin along the Aterno River system and the approximate timing of fluvial integration with their downstream neighbour (see large dark blue arrows). The chronostratigraphic scheme (left side of the figure) was taken from Cohen and Gibbard (2010). Key references are provided below each individual basin column. (1) Early Pleistocene isolation of sub-basins in the MTR basin evidenced by flyschoid and calcareous sediment in the NE and SW sub-basins, respectively. (2) Sub-basin integration caused by sub-basin overfilling evidenced by the appearance of flyschoid gravel in the SW sub-basin. (3) Deep (>40 m) fluvial incision during the early Middle Pleistocene likely related to integration with downstream BPZ basin. Subsequent infilling of incised channels with tephra- and organic-rich sediment. (4) Fluvial sediment with reversed magnetic polarity in the windgap between BPZ and ASB basins suggest a through-going river system to have formed sometime during the Early Pleistocene, however, exact timing of drainage integration is poorly constrained. (5) Aterno River channel has an incised position (up to ~50 m) within Early-Middle Pleistocene sediment, however, the origin (fluvial or fault-related) and age of these terraces are not constrained. (6) Transition from alluvial fan/slope deposits to lacustrine sediment biostratigraphically dated to 2–1.7 Ma. Locally this transition comprises a period of non-sedimentation and soil development (e.g., on abandoned fan surfaces and fault-related terraces). (7) Rock avalanche activity may explain the differences between the late Middle Pleistocene-Recent stratigraphies in ASB basin areas up- and downstream of L'Aquila. (8) Lake disappearance in the PSD basin estimated to ca. 0.8–0.7 Ma based on developments in the adjacent LAS and Castelnuovo basins (see main text). (9) Lacustrine sedimentation first followed by fluvial sedimentation in the PSD basin. However, the PSD basin may have experienced a short period of (minor) fluvial incision or non-deposition during the early Middle Pleistocene (Giaccio et al., 2012). (10) We suspect at least part of the terrace morphology in the downstream part of the PSD basin to be related to the wave of erosion propagating upstream from the San Venanzio gorge. (11) Lacustrine silts grade upwards into fluvial gravels showing reversed flow direction towards the PSD basin. Around 0.7 Ma, a fluvial connection through the San Venanzio gorge and a normal flow direction across the LAS basin were established, followed by the onset of strong fluvial incision. (12) Top of the Early to early Middle Pleistocene lacustrine unit (unit 'SUL6' according to Giaccio et al., 2013) estimated to ca. 650 ka, assuming a constant sedimentation rate and extrapolating from a $^{40}Ar/^{39}Ar$ dated tephra layer from ca. 724 ka (Zanchetta et al., 2017). (13) First main phase of incision in the Sulmona basin, with soil development on the abandoned terraces. End of this phase is well constrained by a thick 527 ka tephra layer observed directly above the palaeosol (Zanchetta et al., 2017). (14 and 15) Strong aggradation between ca. 530 and 135 ka, causing the deposition of lacustrine sediment in the downstream part of the basin (near the Popoli gorge) and > 50 m of fluvial gravel across the remaining part of the basin (Miccadei et al., 2002). (16) Around 135 ka, a second main phase of incision started in the Sulmona basin, however, which was periodically affected by travertine formation within and downstream of the Popoli gorge (Lombardo et al., 2001) (17) Temporal re-establishment of underfilled / lacustrine conditions during the late Middle Pleistocene in the Bazzano sub-basin (e.g., Macri et al., 2016).

Stratigraphic cross-sections across the ASB, PSD, LAS and SUL basins
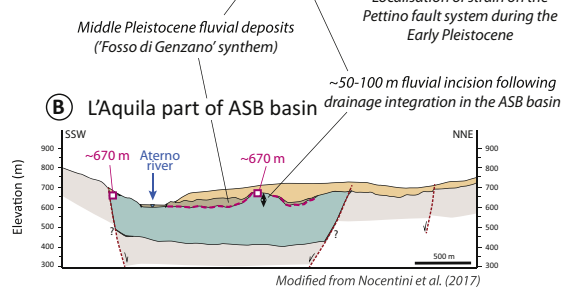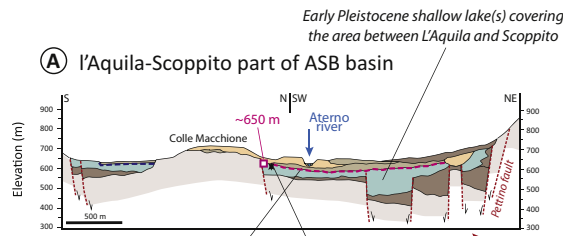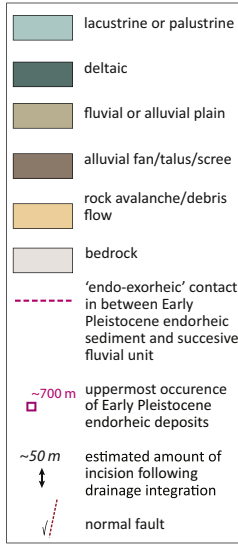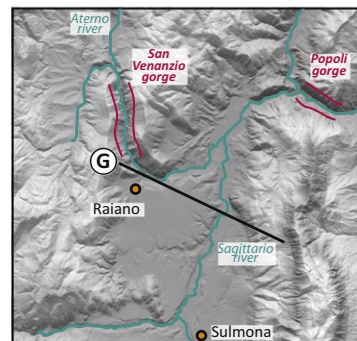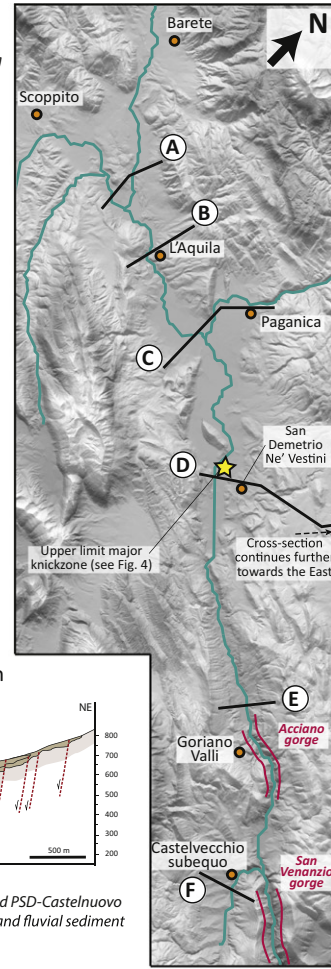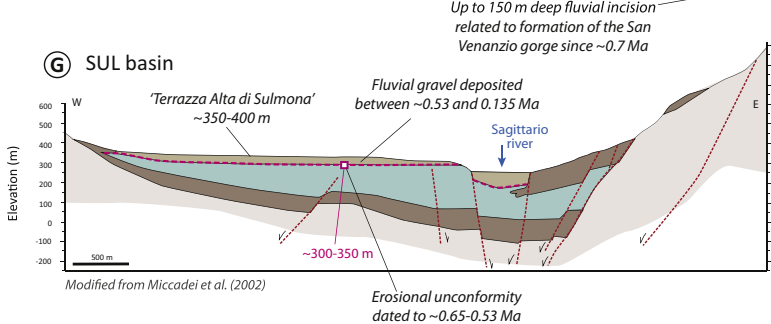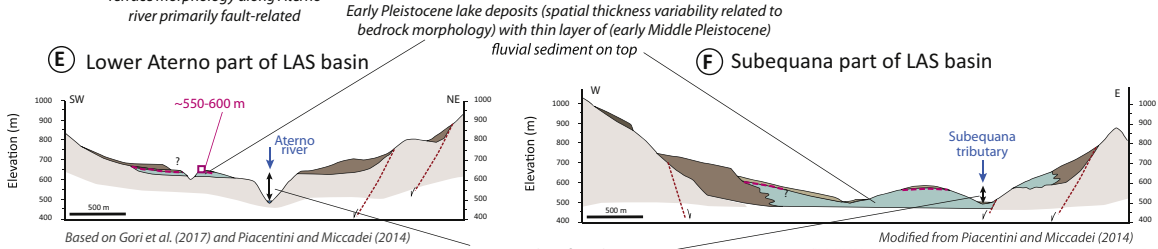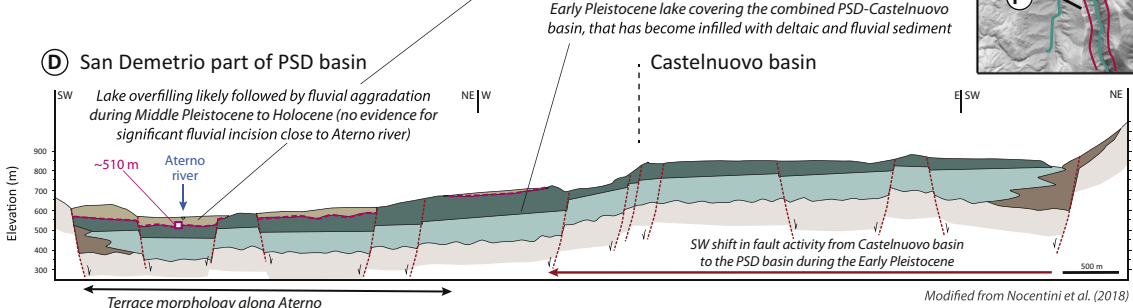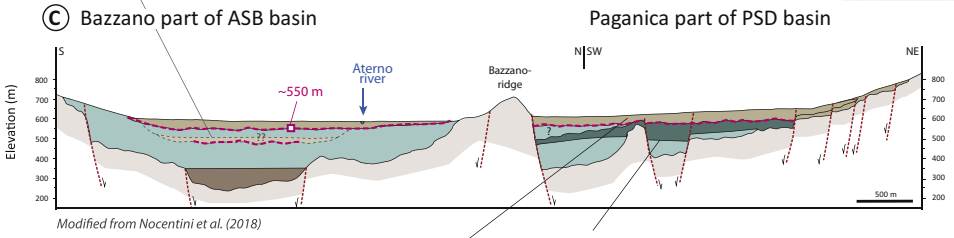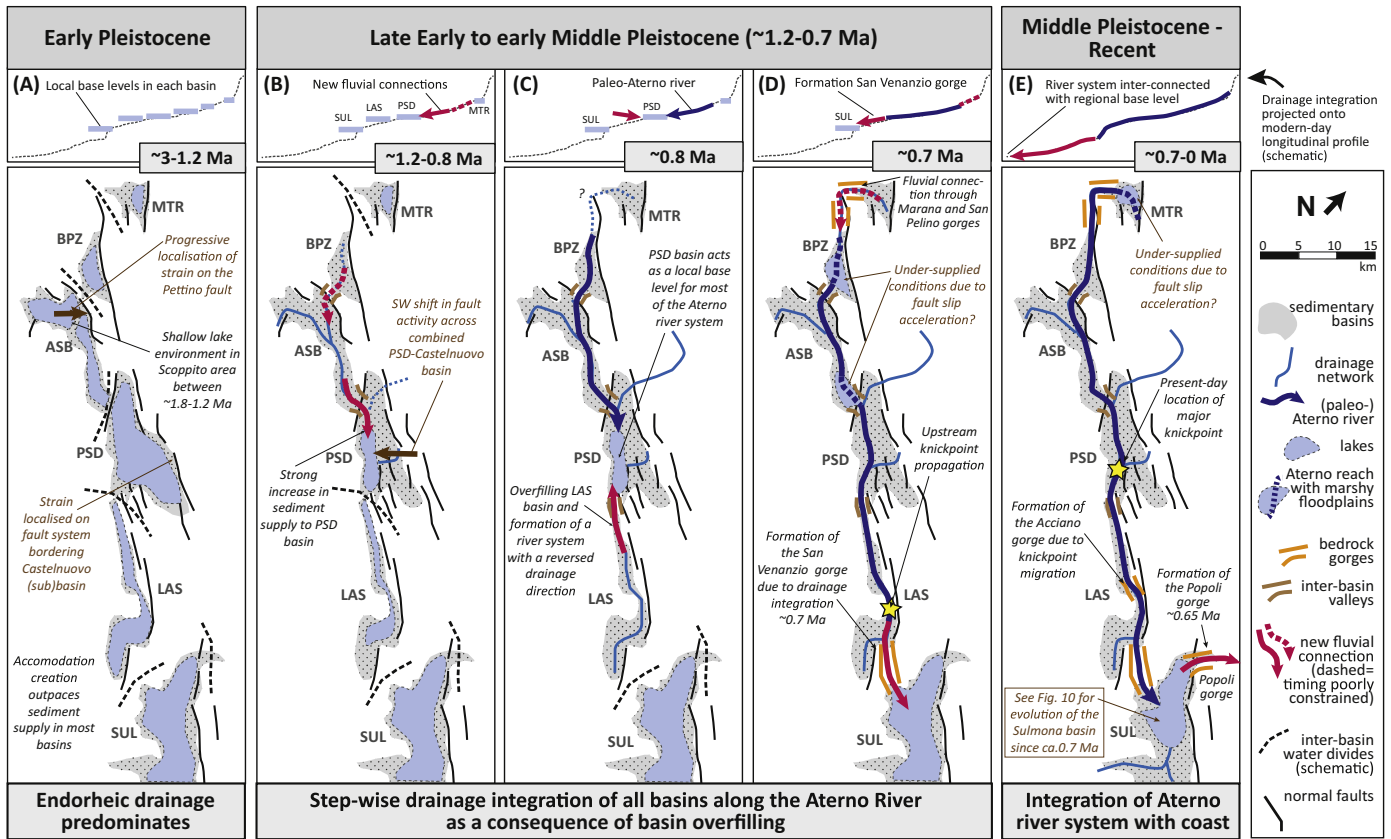
Fig. 8. Palaeogeographic maps showing the development of the Aterno River system for different time intervals as described in the main text (bottom panels). The long-term trend of drainage integration is also (schematically) projected onto the longitudinal profile of the Aterno River (top panels). (A) All basins were isolated from one another and supported lakes during the greatest part of the Early Pleistocene (ca. 3–1.2 Ma). (B), (C), and (D): Between ca. 1.2 and 0.7 Ma, all basins along the Aterno River became step-wise integrated with one another. Drainage integration started in the area around L'Aquila and occurred because of basin filling and overflow caused by an increase in sediment (and water) supply relative to basin subsidence (see also Fig. 9). (E) Approximately 0.65 Ma, a fluvial connection between the fully integrated Aterno River system and the Adriatic foreland became established (see also Fig. 10).

additionally experienced major rock avalanche and debris flow events in the L'Aquila-Colle Macchione area (Figs. 3A, 4A, and 6, and see yellow units in cross sections A and B in Fig. 7; Nocentini et al., 2017). The Pettino Fault is the main basin-bounding fault system and is inferred to have a Holocene slip rate of approximately 0.6 mm yr^{-1} (Galli et al., 2011).

In the PSD basin, no clear evidence exists for significant fluvial incision adjacent to the Aterno River directly following drainage integration around 0.7 Ma (Fig. 6; Giaccio et al., 2012). In this basin, ~50 m of fluvial sediment was deposited on top of the Early (to early Middle) Pleistocene lacustrine deposits during the Middle to Late Pleistocene time interval (Nocentini et al., 2018). Most of the relief in the PSD basin can be explained by activity on the large number of normal fault segments that together control basin subsidence (Fig. 3A, cross section D in Fig. 7). However, in the most downstream part of the basin, downstream of San Demetrio Ne' Vestini, some of the terrace morphology may additionally relate to the wave of incision propagating upstream from the San Venanzio gorge and LAS basin (Fig. 4A and C). Middle

Pleistocene to present-day slip rate estimates for the main fault system controlling the PSD basin are of the order of ~0.5–0.7 mm yr^{-1} (Galli et al., 2010, 2011; Moro et al., 2013).

In the LAS basin, drainage integration was followed by intense fluvial incision caused by the large drop in local base level caused by incision of the San Venanzio gorge (Figs. 4A, C, 5A, and 6, and cross sections E and F in Fig. 7; Gori et al., 2015, 2017). Incision is still on going and has so far produced around 100–150 m of incision in the downstream part of the LAS basin (Fig. 4A and cross sections E and F in Fig. 7) and limited incision (<20–30 m) in the upstream part of the LAS basin (Fig. 4A). Maximum Holocene throw rate along the main basin-bounding fault system is estimated to be in between 0.3 and 0.7 mm yr^{-1} (Galadini and Galli, 2000; Faure Walker, 2010).

In the SUL basin, 50–100 m of aggradation occurred between ca. 530 and 135 ka mainly comprising gravels (Miccadei et al., 2002; Giaccio et al., 2009, 2013; Zanchetta et al., 2017). However, in the most downstream (northeastern) part of the basin, mainly lacustrine sediment is observed (Zanchetta et al., 2017). From ca. 135 ka onwards, the Aterno

Fig. 7. Stratigraphic cross sections through the four most downstream located ASB, PSD, LAS and SUL basins (references provided underneath each cross section). Transect positions are also shown in Figs. 3A and 4A. With pink lines, we marked the contact between the pre-drainage integration endorheic (lacustrine/palustrine/deltaic) sediment and the post-drainage integration fluvial sediment. The pink squares show the uppermost elevation of this contact that we use in Fig. 4A. Cross sections A and B and the southern part of C cross the ASB basin. The Early Pleistocene to early Middle Pleistocene parts of these cross sections are similar. However, cross sections A and B show the 50–100 m thick late Middle Pleistocene rock avalanche deposits (in yellow), while cross section C shows a late Middle Pleistocene lacustrine unit (e.g., Macri et al., 2016). Cross section D and the northern part of cross section C show the stratigraphy of the PSD basin. Characteristic for the PSD basin are the up to 100 m thick deltaic deposits overlying the lacustrine unit. While the Early Pleistocene lake covered both the PSD basin and Castelnuovo sub-basin, Middle Pleistocene fluvial activity was limited to the PSD basin from the Middle Pleistocene onwards caused by a SW shift in fault activity (see cross section D). Cross sections E and F cross the LAS basin. They show the variability in thickness of the Early Pleistocene lacustrine sediment along the basin and the thin layer of overlying fluvial deposits related to overfilling of the basin ca. 0.8 Ma. They also show the up to 150 m deep incision that as occurred since the formation of the San Venanzio gorge ca. 0.7 Ma. Cross section G crosses the SUL basin, and shows the thick sequence of Early to Middle Pleistocene (>0.65 Ma) lacustrine sediment, with on top the ~50 m layer of (ca. 530–135 ka) fluvial gravel.

River has been mainly incising, adjusting its profile in response to base level fall across the Popoli gorge. The maximum Holocene throw rate estimated for the basin-bounding Monte Morrone/Sulmona fault system is approximately 1.1 mm yr^{-1} (Roberts and Michetti, 2004), suggesting a significant acceleration in fault slip rate during the Middle Pleistocene.

5. Evolution of the Aterno River system in response to drainage integration

The dominant stratigraphic trend observed in all six basins is a transition from primarily lacustrine to fluvial sedimentation that is interpreted to record the progressive integration of the drainage network along the Aterno River system (Fig. 8). Long-term drainage integration in the central Apennines has previously been described (e.g., D'Agostino et al., 2001; Bartolini et al., 2003; Piacentini and Miccadei, 2014) and reproduced by means of numerical modelling (Geurts et al., 2018). However, the data compilation for the Aterno River reported here provides detailed insights into the timing, variable character and causes of the individual drainage integration events.

The timing of drainage integration is not a function of distance from the coast (Fig. 8). Based on the available evidence, it appears that drainage integration commenced along the middle reaches of the Aterno River system, in the ASB or BPZ basin, and occurred last between the most downstream located SUL basin and the Adriatic coast. Consequently, the spatio-temporal pattern of drainage integration is not consistent with a model where progressive hinterland capture is driven by headward erosion from the coast (e.g., D'Agostino et al., 2001; Dickinson, 2015). As demonstrated by numerical modelling experiments (Geurts et al., 2018) and suggested by drainage integration studies focussing on other areas (e.g., Connell et al., 2005), the more disordered pattern of drainage integration that we observe for the Aterno River could be expected from overspill mechanisms, i.e., the overfilling of basins with sediment and water (Geurts et al., 2018). We come back to this in more detail in Section 6.1.

We interpret the three large-scale convexities along the Aterno longitudinal profile to relate to the progressive, long-term integration of the drainage network (Fig. 4B). For all of these convexities, we can exclude a lithology or fault-related origin. We therefore interpret them as transient features reflecting the ongoing adjustment of newly established fluvial connections between initially isolated basins (Fig. 1C). Moving in a downstream direction, we explain the three major knickzones along the Aterno River profile to reflect integration events between the MTR and BPZ basins, between the LAS and SUL basins, and between the SUL basin and the Adriatic foreland (Miccadei et al., 2002; Giaccio et al., 2013; Chiarini et al., 2014; Gori et al., 2017). As these knickzones migrate upstream, they cause incision into the endorheic deposits of the upstream basin fill and terrace formation (Figs. 1C and 4A). The best examples are the substantial terraces within the LAS basin, which have surface elevations up to 150 m above the present-day Aterno River (Fig. 5A). Even though incision is observed in most basins, it is important to note that this does not represent a single wave of erosion, but multiple waves that started at different times in the individual basins.

The transition from internal (endorheic) to external (exorheic) drainage evidently led to a shift from the complete storage of sediment within individual basins towards the partial reworking and export of sediment towards other basins downstream or the Adriatic coast. The export of sediment explains the relatively low thickness of fluvial sediment (of late Early Pleistocene to Recent age) compared to their lacustrine (Early to early Middle Pleistocene) counterparts, taking into account the different duration of the time intervals during which these deposits were formed (Fig. 7).

While drainage integration is the dominant long-term trend for the basin evolution along the Aterno River over the last ~3 Myr, the younger stratigraphy of some basins shows intervals that record a transition back from fluvial to lacustrine or to palustrine depositional environments (Fig. 6). Examples of these fluvial to lacustrine/palustrine transitions occur in the MTR basin (Chiarini et al., 2014), the BPZ basin (Bosi et al., 2004), the Bazzano part of the ASB basin (Macri et al., 2016; Porreca et al., 2016), and the northeastern part of the SUL basin (Giaccio et al., 2013; Zanchetta et al., 2017). These transitions provide evidence that these basins must have become at least partly underfilled during the Middle to Late Pleistocene or Holocene.

6. Discussion

The data compilation presented in this paper shows the progressive integration of basins along the Aterno River in the actively extending central Italian Apennines. Here we first discuss the factors that likely primarily controlled the evolution of the Aterno River (Section 6.1) and describe the variability in which drainage integration events are expressed in the stratigraphic-geomorphological records of the different basins (Section 6.2). Subsequently, we evaluate how long it takes for the landscape to respond to long-term drainage integration (Section 6.3), and discuss the general implications of our work in terms of the importance of drainage network evolution for transient landscape evolution and basin stratigraphy in continental rifts (Section 6.4).

6.1. Potential controls on drainage integration

Factors that controlled the fluvial connectivity between neighbouring extensional basins along the Aterno River are those that can modify the balance between the rate of water supply, sediment supply and the rate of basin subsidence and can in turn cause a basin to switch between underfilled and overfilled conditions (Fig. 1B; e.g., Gawthorpe et al., 1994). Where the integrated sediment supply exceeds basin subsidence in volumetric terms, this can cause an endorheic underfilled basin to become overfilled and to form a fluvial connection with its downstream neighbour. If basin subsidence exceeds sediment supply, on the other hand, a fluvially integrated basin may return to underfilled or even endorheic conditions (e.g., Geurts et al., 2018). Further factors that are additionally important are pre-existing topography that sets the height of the spill point, and the water supply-to-evaporation ratio that controls lake levels (Fig. 1B).

Overspill mechanisms are inferred to have controlled drainage integration in other continental extensional settings such as along the Rio Grande (e.g., Connell et al., 2005; Repasch et al., 2017), the lower Colorado River downstream of the Colorado plateau (House et al., 2008), the Salt and Verde rivers in Arizona (Larson et al., 2014), and the Amargosa, Owens, and Mojave rivers in Nevada-California (Meek, 1989, 2019; Menges, 2008; Phillips, 2008). In the central Apennines, the importance of the interplay between sediment supply, water supply and basin subsidence in controlling drainage network evolution has only been suggested at the scale of individual hangingwall basins (e.g., Mancini et al., 2012; Chiarini et al., 2014; Macri et al., 2016). We believe, however, that shifts in balance between sediment supply, water supply and basin subsidence can explain many observations from the Aterno River system as a whole, and for the central Apennines in general.

6.1.1. Underfilled conditions during the Early to early Middle Pleistocene

We expect the prevailing trend of drainage integration along the Aterno River to result from a long-term increase in sediment supply relative to basin subsidence, allowing the initially isolated basins to overspill. We test this idea in Fig. 9 by generating estimates for the accumulation of basin subsidence and hangingwall sediment thicknesses for basins along the Aterno River. During early stages of extension, faults in the central Apennines are estimated to have had throw rates of the order of 0.3–0.35 mm yr^{-1} (Roberts and Michetti, 2004). When assuming typical long-term ratios of footwall uplift to hangingwall subsidence in the range of 1:1 to 1:2 (e.g., Bell et al., 2018; De Gelder et al., 2019) these values would correspond to 0.15–
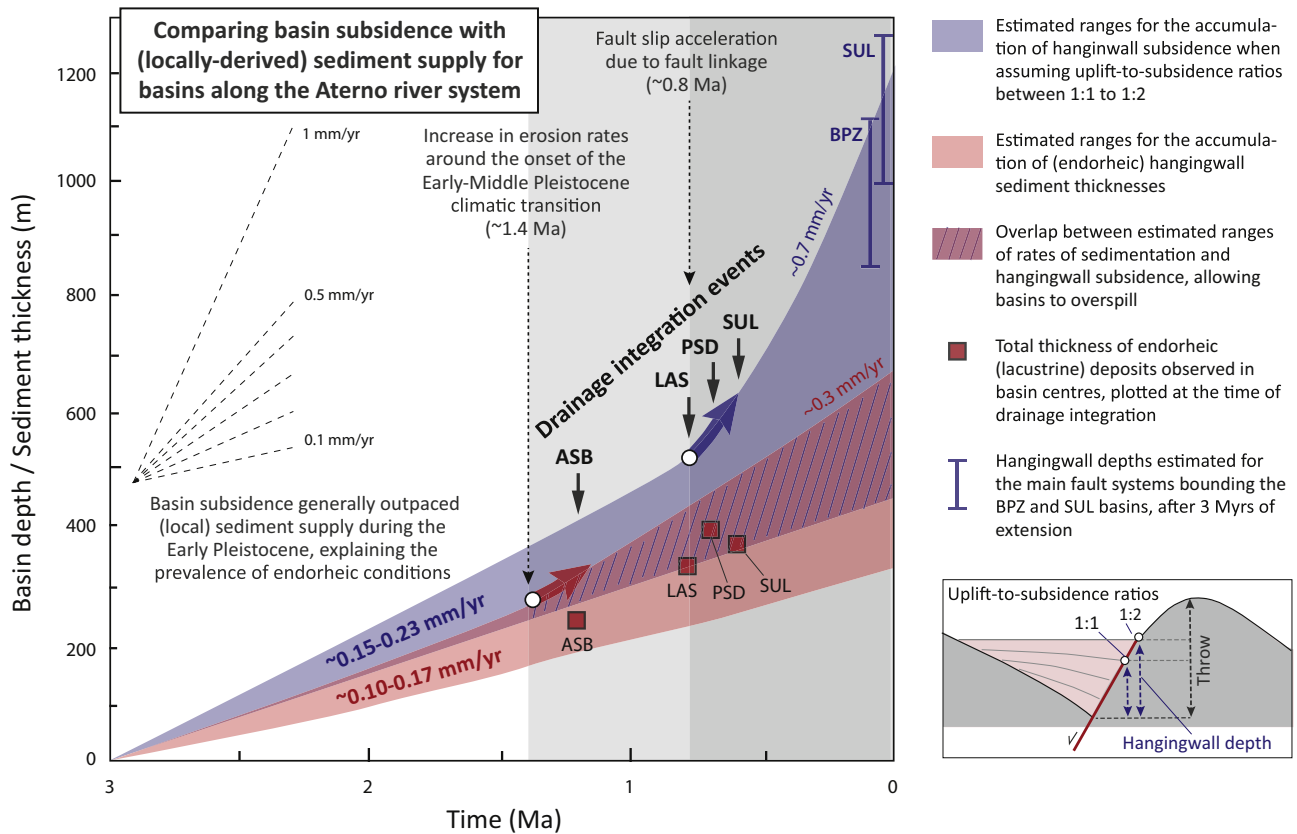
Fig. 9. The progressive accumulation of basin subsidence (blue shading) and hangingwall sediment thickness (red shading) based on fault slip rate, total throw and stratigraphic data compiled for the basins along the Aterno River and the main basin-bounding faults (see main article text for explanation). When assuming typical long-term ratios of footwall uplift to hangingwall subsidence in the range of 1:1–1:2, we expect approximately half to two-thirds of the accumulated fault throw to represent the basin volume that is available for sediment to accumulate (see inset figure and main text). Basin subsidence outpaced sedimentation during most of the Early to early Middle Pleistocene, explaining the prevalence of endorheic conditions at that time. However, over the long-term we expect sediment supply to have increased because of the progressive increase in fault-related relief and changing climatic conditions related to the Early to Middle Pleistocene climatic transition. Enhanced sediment supply likely led to more overlap between sedimentation and basin subsidence rates (hashed area) and, in turn, to have allowed some basins to overspill. We illustrate the increase in sedimentation rates by means of an approximate doubling of the estimated maximum sedimentation rates from ca. 1.4 Ma onwards (red arrow), however, note that less than a doubling is sufficient to 'tip the balance'. The red squares show the approximate thickness of the sedimentary fills from the central parts of the four southernmost basins at the time of drainage integration. Because part of the endorheic sediment may have been eroded as a consequence of drainage integration events, these thicknesses may have been larger. Fault segment interaction and linkage may have allowed some faults to accelerate their slip rates up to 1.1 mm yr^{-1} around 0.8 Ma (blue arrow), corresponding to a maximum hangingwall subsidence rate of ~0.7 mm yr^{-1} when assuming a uplift-to-subsidence ratio of 1:2. Such acceleration may for some basins explain a part return to palustrine and lacustrine conditions during the Middle Pleistocene to Holocene time interval. In the upper right corner we show the approximate hangingwall depths of the SUL and BPZ basins, based on their total throw estimates and assuming an uplift-to-subsidence ratio of 1:2.

0.23 mm yr^{-1} of accumulating hangingwall volume that could be filled with sediment or water (see blue accumulation curve and inset figure in Fig. 9). Uplift-to-subsidence ratios in between 1:1 and 1:1.6 have also been inferred for normal fault systems in the southern Apennines where extension is also accompanied by regional uplift (Roda-Boluda and Whittaker, 2016, 2017), and we consider the maximum possible value of hangingwall subsidence to be given by a ratio of 1:2.

From the geological cross sections of the ASB, PSD, LAS and SUL basins (Fig. 7), and the available chronology, we estimate long-term average sedimentation rates of the order of 0.10–0.17 mm yr^{-1} for the Early to early Middle Pleistocene lacustrine units (Fig. 9; see Supplementary Materials B for details). These are minimum estimates, as part of the sediment from the endorheic phase may not have been preserved. As a comparison, similar sedimentation rates are suggested by a 0.54 Ma old tephra layer at 100 m depth in the Fucino basin, which is the only large isolated basin that is left in the central Apennines today (Cavinato et al., 2002; Whittaker et al., 2008). A key observation from Fig. 9 is that, during the Early to early Middle Pleistocene, our estimated rates of sedimentation (0.10–0.17 mm yr^{-1}) are generally less than the initial rates of hangingwall subsidence (0.15–0.23 mm yr^{-1}). Even though there is some uncertainty in these estimated ranges, which can differ between the individual basins, the difference in rates is

consistent with basins in the central Apennines being predominantly underfilled and isolated during the Early (to early Middle) Pleistocene (Fig. 9; e.g., D'Agostino et al., 2001; Piacentini and Miccadei, 2014).

6.1.2. Tipping the balance between basin subsidence and 'local' sediment and water supply

The small difference between the estimated rates of sedimentation and basin subsidence during the Early Pleistocene suggests that only small increases in sediment supply would have been needed to have tipped the balance towards oversupplied conditions and to allow basins to overspill. This is exactly what we interpret to have occurred for the ASB and BPZ basins that were most likely the first basins to become integrated during the late Early Pleistocene (Figs. 6 and 8). We expect sediment supply to have increased progressively over time, first because of the long-term increase in fault-related topography (Geurts et al., 2018). Second, there was a shift towards more prolonged and intense glaciations during the Early to Middle Pleistocene climatic transition (ca. 1.4–0.4 Ma; Head and Gibbard, 2015). We know that in the central Apennines, glacial conditions strongly enhanced erosion and runoff, so sediment supply is likely to have increased from approximately 1.4 Ma when glacial periods became longer and more intense (Giraudi and Frezzotti, 1997; Tucker et al., 2011; Whittaker and Boulton, 2012).

Weathering rates, erosion rates, and runoff have been inferred to have been 30, 10, and 4 times higher, respectively, under glacial conditions compared to interglacial conditions in the central Apennines (Whittaker et al., 2010; Tucker et al., 2011; Whittaker and Boulton, 2012). We depict a conservative increase of ~2 times (corresponding to a sedimentation rate of ~0.3 mm yr^{-1}) to illustrate the increase in sediment supply in Fig. 9 from the onset of the Early to Middle Pleistocene climatic transition (ca. 1.4 Ma; Head and Gibbard, 2015). Fig. 9 shows that such a doubling in sedimentation rates is more than sufficient to significantly enhance the overlap (see hashed area in Fig. 9) between the estimated ranges of the rates of sedimentation and hangingwall subsidence. Even though these are first-order estimates, it seems a plausible scenario that an increase in sediment (and water) supply around the Early to Middle Pleistocene climatic transition has allowed sedimentation rates in some basins to have matched or overtaken fault-driven hangingwall subsidence, causing them to overspill, and the long-term trend of drainage integration to commence.

6.1.3. The role of enhanced down-system sediment and water transport during drainage integration

As soon as overspilling of the ASB basin and BPZ basin had led to establishment of a through-going river system connecting these adjacent basins, sediment and water were no longer trapped within these basins and could be transported down-system. This means that for those basins located downstream, the balance towards overfilled conditions could, from now onwards, additionally be tipped by increased sediment and water discharge derived from the significantly larger upstream drainage catchment area. The down-system transport of sediment and water across different basins tends to trigger drainage integration in basins located farther downstream, extending the length of axial river systems in a top-down direction. Meek (2019) discusses this conceptual model in more detail and provides an overview of supporting field evidence from different river systems in the western United States. In the Aterno River system, this model can for instance explain the sudden increase in sediment supply to the PSD basin around 1.2–1.1 Ma (dark blue deltaic unit in cross sections C and D in Fig. 7; Giaccio et al., 2012; Nocentini et al., 2018). This increase in sediment supply led to fast progradation of delta systems, particularly from the northern side of the basin, which coincides with lake disappearance and the onset of incision directly upstream in the ASB basin (Mancini et al., 2012; Nocentini et al., 2017). Drainage integration between the ASB and PSD basins increased the source area of the PSD basin by a factor of ~2.5 to 3.5 times (depending on whether the ASB was already integrated with the BPZ basin before that time), generating a large amount of sediment both by erosion of the larger upland area as well as by fluvial incision into the ASB basin (and perhaps also the BPZ basin) infill. This in turn could lead to enhanced sediment input into the PSD basin and enhanced rates of delta progradation into the large Early Pleistocene lake.

Another observation that suggests an important role for up-system derived sediment and water is the timing of formation of the Popoli gorge around 0.65 Ma (Giaccio et al., 2013; Zanchetta et al., 2017), which is shortly after the formation of the San Venanzio gorge (ca. 0.7 Ma; Gori et al., 2015, 2017). Drainage integration across the San Venanzio gorge led to a dramatic increase in upstream contributing area to the SUL basin with ~1300 km^2 (size of the Aterno River catchment). Although there is no definitive stratigraphic evidence, we hypothesise that this drainage integration event likely caused significant deepening of the lake in the SUL basin around 0.7–0.65 Ma (Fig. 10) caused by the significantly increased water discharge. Considering the position of SUL basin at the very end of the Aterno River system and the timing of drainage integration across the San Venanzio gorge during one of the most extreme glacial periods (MIS16), we might expect this lake to have had at least the volume of the large Early Pleistocene lake in the PSD basin (e.g., Giaccio et al., 2012). We
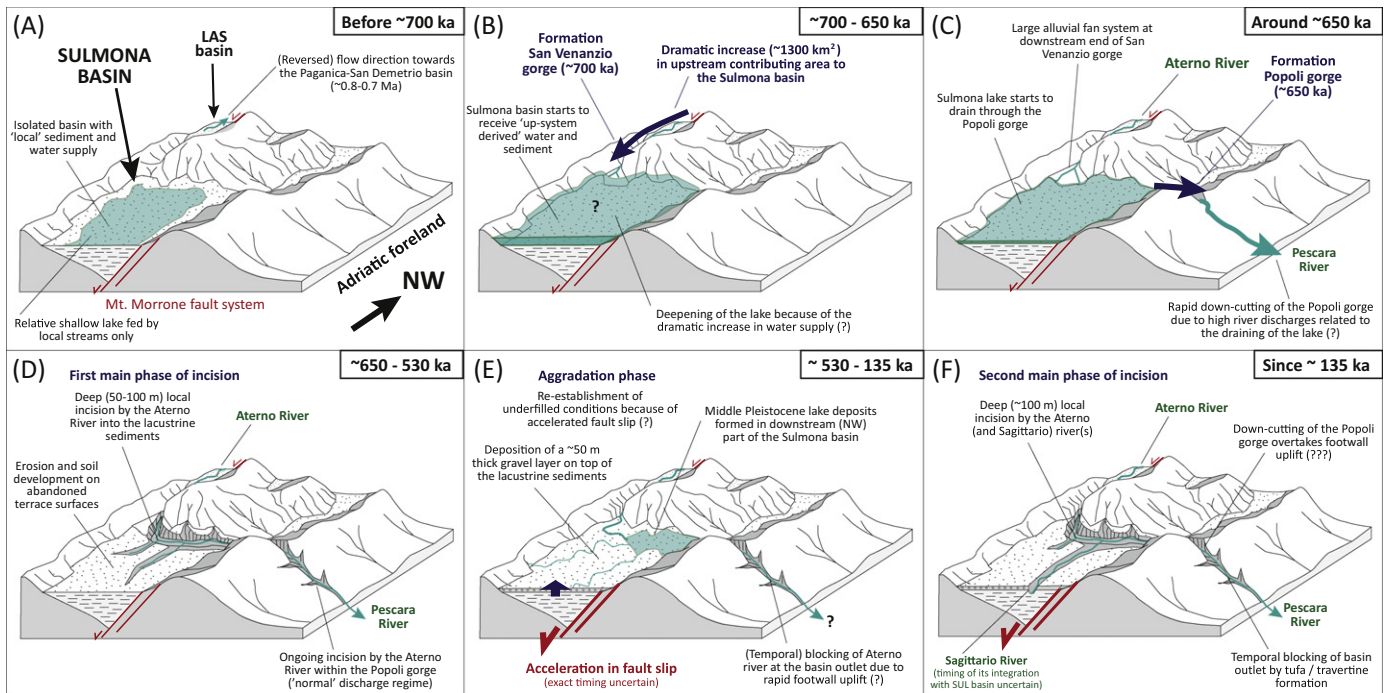
Fig. 10. Palaeogeographic and tectono-sedimentological reconstruction for the Sulmona basin (looking towards the west). (A) During the Early (to early Middle) Pleistocene, the Sulmona basin was an endorheic basin, fully isolated from the upstream Aterno River system and the Adriatic foreland area. (B) Around 700 ka, overspill of the LAS basin led to the integration of the Aterno River catchment with the Sulmona basin (Gori et al., 2015, 2017). We hypothesise that this drainage integration event produced a dramatic increase in water supply and in turn led to significant deepening of the lake. (C) The emptying of this lake may have had an important role in the formation of the Popoli gorge around 650 ka. (D) Drainage integration across the Popoli gorge produced an upstream propagating wave of (local) fluvial incision between ca. 650 and 530 ka (Zanchetta et al., 2017). (E) Fault slip acceleration can (at least partly) explain the re-establishment of undersupplied conditions between ca. 530 and 135 ka, and the deposition of 50–100 m thick fluvial gravel and lacustrine deposits. (F) Since ca. 135 ka, the Sulmona basin has been mainly affected by fluvial incision, however, during this time interval sedimentation has been additionally affected by tufa or travertine formation in the area of the Popoli gorge (Lombardo et al., 2001).

suggest that the emptying of this lake may have had a prominent role in the formation of the Popoli gorge ca. 0.65 Ma (Fig. 10) and may have contributed to the basin-wide erosion that is observed into the top of the Early to early Middle Pleistocene lacustrine unit (Miccadei et al., 2002). Because a deep lake in the SUL basin likely existed for a relative short period of time only, there may not have been sufficient time to deposit stratigraphic features such as the large prograding delta systems observed in the PSD basin. In turn, this might explain why enhanced lake levels in the SUL basin around 0.7–0.65 Ma have not been fully discussed before.

6.1.4. Re-establishment of underfilled conditions during the Middle Pleistocene to Holocene

Fault segment interaction and linkage are documented to have allowed some faults to accelerate their slip rates at approximately 0.8 Ma (Roberts and Michetti, 2004; Whittaker et al., 2007) and can explain why Holocene throw rate estimates for faults bounding the basins along the Aterno River system reach up to 1.1 mm yr^{-1}. This means that an increase in fault-driven basin subsidence of up to 3 times can be expected to have occurred around 0.8 Ma (Fig. 9). Of course, such an increase is not expected for all faults – some faults might have kept a constant slip rate or might even have become inactive. We thus consider a 3 times increase in fault-driven basin subsidence as an upper limit, corresponding to a maximum rate of ~0.7 mm yr^{-1} assuming a footwall uplift to hangingwall subsidence ratio of 1:2 (Fig. 9).

Such an increase in fault slip rate may have led to re-establishment of underfilled lacustrine and palustrine conditions in some of the basins along the Aterno River during the Middle or Late Pleistocene, caused by hangingwall subsidence outpacing sediment supply (Fig. 9). However, it is important to note that Fig. 9 only shows the 'local balance' and does not account for the amount of 'up-system derived' sediment originating from the Aterno River catchment upstream. In case of the MTR basin, however, we can exclude significant upstream drainage area enlargement, as it is the most upstream located basin within the Aterno River system. Therefore, for the MTR basin, it is a plausible scenario that acceleration in basin subsidence may have tipped the balance back to undersupplied conditions in the course of the Middle Pleistocene, explaining a renewed phase of lacustrine and palustrine sedimentation (Fig. 6). Also, in the case of the next basin downstream, the BPZ basin, the reconstructed strong increase in slip rate of the main basin-bounding fault (Roberts and Michetti, 2004; Galli et al., 2011) may be responsible for the re-appearance of lacustrine conditions during the Middle Pleistocene (Bosi et al., 2004; Piacentini and Miccadei, 2014).

A different scenario, however, may apply to the more downstream basins where the contribution of 'up-system derived' sediment was likely much larger, such as the ASB and SUL basins. In these downstream basins, the re-establishment of underfilled conditions may have required other processes, in addition to accelerated basin subsidence driven by increased rates of faulting. For instance, mass wasting events may have played a role in the case of the ASB basin (e.g., Nocentini et al., 2017; Figs. 6 and 7) and in the SUL basin, tufa or travertine formation within and directly downstream of the Popoli gorge may also have influenced sedimentation upstream (Lombardo et al., 2001). While we do not exclude the possibility that the re-establishment of underfilled conditions may have coincided with the temporal damming of the Aterno River, we do not have any evidence suggesting prolonged disintegration of the Aterno River system after it was formed.

6.2. Variable expression of drainage integration events between basins

A key feature of our data is the variability of expression of each drainage integration event in the sedimentological and geomorphological record of the basin. To some extent, this variability can be explained by the difference in timing at which drainage integration occurred. The longer ago that drainage integration occurred, the more time has been

available for the river system to adjust, for instance, in terms of knickpoint propagation. The ASB basin, for example, was likely the first basin that became integrated to its downstream neighbour ca. 1.2–1.1 Ma, resulting in 50–100 m deep dissection of its Early Pleistocene lacustrine deposits. However, around ca. 0.6 Ma, the river had largely adjusted to the fall in local base level and a new phase of fluvial aggradation commenced in response to basin subsidence. The more recently integrated LAS basin (ca. 0.7 Ma), on the other hand, is still adjusting to its fall in local base level.

Another key factor influencing the sedimentological and geomorphological expression of drainage integration is the elevation difference between adjacent basins prior to drainage integration. This determines the magnitude of base level fall experienced by the overspilling basin. For instance, the LAS and SUL basins experienced a large fall in base level (>150 m) that triggered a wave of fluvial incision that deeply dissected the upstream basin forming a pronounced incised valley system (Miccadei et al., 2002; Gori et al., 2017). Because such a large fall in base level leads to the formation of deep gorges and high terrace morphology, this type of drainage integration event is relatively easily observed and tends to receive most attention (e.g., Geurts et al., 2018). In the PSD basin, on the other hand, fluvial erosion following drainage integration seems to have been limited or absent (Fig. 6; Giaccio et al., 2012). Here, aggradation could either continue or rapidly resume because drainage integration occurred simultaneously for the PSD basin and its downstream neighbour, i.e., the LAS basin, which had similar surface elevations, around 0.7 Ma (Fig. 8C and D). Consequently there was only one major fall in base level downstream of the LAS basin, which initially did not affect the PSD basin because the wave of erosion had to migrate across the LAS basin first (Fig. 8D).

Besides the timing of drainage integration and the magnitude of base level fall there are many more factors that we believe have contributed to the pronounced variability of expression of the different drainage integration events in the different basins. For instance, we also expect the size of the drainage system that is upstream to be of major importance because this determines how much additional sediment and water a basin will receive from upstream. Another factor is the size of the lake or the degree of infilling prior to drainage integration. Overspill of basins with large lakes leads to the abrupt dissection of fine-grained lacustrine sediment (e.g., the ASB and SUL basins) while in basins that are (almost) filled, the fine-grained lacustrine unit is already largely topped by coarse-grained fluvial or deltaic sediment (e.g., the LAS and PSD basins). The data from the Aterno River system would therefore allow for a future comparison of the exact expression of the different drainage integration events given these constraints.

6.3. Landscape response times

Our data compilation shows the step-wise development of the Aterno River through a series of drainage integration events (Fig. 8). If extension started around 3 Ma, it took ~2.4 Myr in total for this axial river system to develop its course down to the SUL basin, and to form a connection between this most downstream located basin and the Adriatic coast. Even though the river is now fully integrated, its longitudinal profile suggests that it is far from topographic steady state and is still adjusting to the drainage integration events from which it was formed (Fig. 4).

The horizontal distance along the largest convex reach (30–35 km), i.e., the one upstream of the Sulmona Basin (Fig. 4B), suggests an average knickpoint migration rate of the order of 43–50 mm yr^{-1} since drainage integration occurred ca. 0.7 Ma, assuming the upper limit of the knickpoint at an elevation of 575 m is the farthest that the signal of this drainage integration event has propagated. Assuming a unit stream power model and normalising this rate by the square root of drainage area, gives a normalised knickpoint migration rate parameter of 1.4–1.7·10^{-6} yr^{-1} following the approach of Whittaker and Boulton (2012; see Supplementary Materials C for details). This value of

knickpoint propagation rate overlaps with the upper end of the spectrum of values that have previously been calculated for footwall catchments in the central Apennines that are adjusting to an increase in fault slip rate (0.2–2·10^{-6} yr^{-1}; Whittaker and Boulton, 2012), but is a factor of 5 to 7 times lower than the value of 1×10^{-5} yr^{-1} quoted by Loget and Van den Driessche (2009) for knickpoint migration in European catchments during the Mediterranean salinity crisis where the maximum base level change was ~1.5 km. Relatively fast migration rates along the Aterno River relative to footwall catchments in the central Apennines may be explained by the occurrence of relative easily erodible basin sediment compared to the more resistant footwall lithologies and the much larger upstream area of the Aterno River.

Based on our normalised knickpoint propagation parameter of 1.4–1.7·10^{-6} yr^{-1}, we calculate that it would take at least another 3 Myr for the Aterno long profile convexities to become fully eliminated and for the whole catchment to become geomorphically adjusted to river network integration (see Supplementary Materials C). Importantly, this calculation demonstrates that transient conditions can persist for longer following drainage integration than the time period that needed for the river network to become integrated in the first place. We suggest that this effect is under-recognised in stratigraphic and geomorphological studies in normal fault arrays. Moreover, local-scale reversals back to endorheic conditions might be able to 'freeze' or prolong this process of landscape adjustment to drainage integration considerably.

6.4. Drainage network evolution vs. climatic and tectonic forcing

Our data compilation shows that for the greatest part of the total period of extension, i.e., from ca. 3 to ca. 1.2–0.65 Ma, most basins along the Aterno River were isolated from one another. This means that during this time interval, transient climate or tectonic-related signals could not propagate far across the landscape. This has important implications for the interpretation of sedimentary and geomorphological trends observed in the interior of the mountain range. For instance, strong base level fall relative to sea level as a consequence of regional uplift across the central Apennines is generally used for explaining the observation of widespread fluvial incision (e.g., D'Agostino et al., 2001; Bartolini et al., 2003; Giaccio et al., 2012; Chiarini et al., 2014; Gori et al., 2015). However, our dataset shows that the basins associated with the Aterno River were not connected to the coast before ca. 0.65 Ma, and thus fluvial incision in most basins was triggered by a series of local base level falls related to multiple drainage integration events. Because these drainage integration events were initiated at different points in space and time, they need to be considered as individual waves of incision, even though intense incision is a region-wide observed phenomenon at a broad scale.

This study underlines the significant impact of drainage network evolution on transient landscapes and basin stratigraphy. We suggest that the Aterno River system is a strong exemplar of how long-term drainage network integration can be as important as tectonic and climatic forcing in determining the geomorphological and stratigraphic development within extensional settings. Indeed, recent numerical modelling experiments have shown that drainage integration can produce dynamic landscape evolution even if tectonic and climate forcing is held constant (Geurts et al., 2018). Changes in drainage network connectivity can cause marked changes in sediment supply and depositional environments within individual subsiding basins (e.g., Giaccio et al., 2009), for example, causing alternating stages of aggradation and incision, and the formation of fluvial terrace morphology (e.g., Wegmann and Pazzaglia, 2009). However, an important difference, compared to climate-driven changes in sediment supply and depositional environment, is that changes related to climate should affect different basins across a region more or less similarly and simultaneously, even if they are isolated from one another. In contrast, drainage integration can lead to significant variations between neighbouring basins. Drainage

network evolution can also control local base level (e.g., Duffy et al., 2015; Gawthorpe et al., 2018) and can force landscapes to respond to a fall in relative base level by means of upstream propagating waves of erosion (e.g., Whittaker et al., 2007, 2008). However unlike tectonic forcing on individual catchments, the timing and magnitude of the base level fall does not have to correlate directly with the initiation or change in slip rate on a fault. Because of the strong tectonic activity in the central Apennines (and in other normal fault arrays), both at a regional and fault-block scale, stratigraphic and geomorphological observations tend to be mostly approached in terms of tectonic developments (e.g., D'Agostino et al., 2001; Bartolini et al., 2003; Whittaker et al., 2010; Giaccio et al., 2012; Chiarini et al., 2014; Gori et al., 2015) while the contribution of drainage integration along the large axial rivers tends to be overlooked. Our study strongly challenges this assumption.

7. Conclusions and implications

This paper synthesises geomorphological and basin stratigraphic data for a large axial river system in the central Apennines —the Aterno River system —in order to reconstruct its development during the time of active extension (since ca. 3 Ma). We use these data to reconstruct drainage network evolution and evaluate how drainage integration controls transient landscape development and basin stratigraphy. Our main conclusions are:

1) We observe a long-term trend of drainage integration along the Aterno River, evidenced by a transition from predominantly lacustrine to fluvial sediment in all basin stratigraphic records. All basins were internally drained during the Early (to early Middle) Pleistocene and have become fluvially integrated with one another and the Adriatic coast between ca. 1.2 and 0.65 Ma. Consecutive drainage integration events produced discrete waves of fluvial incision and terrace formation.

2) Basins with an intermediate location along the Aterno River, around the city of L'Aquila, likely became fluvially integrated with one another first. Drainage integration occurred last between the most downstream located Sulmona basin and the Adriatic foreland. This spatio-temporal pattern of drainage integration is not consistent with a pattern that would be expected from upstream-directed headward erosion from regional base level (e.g., D'Agostino et al., 2001).

3) The spatio-temporal pattern of drainage integration can be explained by an increase in sediment and water supply relative to hangingwall subsidence that caused basins to overspill. On average, rates of sedimentation were lower than rates of hangingwall subsidence during most of the Early to early Middle Pleistocene, explaining why all basins were endorheic at that time. However, because the difference between sedimentation and throw rates was minor, only a small increase in sediment and water supply was sufficient to tip the balance towards oversupplied conditions.

4) The increase in sediment and water supply relative to basin subsidence is explained by the Early to Middle Pleistocene climatic transition and the progressive increase in fault-related relief. As soon as the first basins were integrated, enhanced sediment and water supply additionally resulted from the marked increase in upstream contributing area.

5) Acceleration of slip caused by fault interaction and linkage around 0.8 Ma can explain the re-establishment of palustrine and lacustrine conditions during the Middle Pleistocene to Holocene time interval for some basins along the Aterno River. However, no evidence exists for the full disintegration of the river system during this time.

6) Overall, we conclude that rates of sedimentation and hangingwall subsidence in the central Apennines are well-matched, allowing tipping points between over- and underfilled conditions to be easily reached.

7) Our data show that the step-wise integration of the drainage network took over 2 Myr, and our calculations indicate that the response time for the Aterno River to re-equilibrate following complete drainage integration is at least 3 Myr. Consequently the effects of drainage network evolution can persist in landscapes and sediment routing systems for significant periods following complete integration of the fluvial system.

8) A broader implication of this work is in elevating the importance of the evolution of fluvial connectivity in continental rifts to the level of tectonics and climate in controlling transient landscape evolution and basin stratigraphy. Drainage network evolution in continental rifts is often considered as a simple consequence of tectonics, and in some cases climate change. This study suggests that drainage integration between individual rift basins be looked upon as an important factor in its own right. While drainage network evolution receives a lot of attention in settings where tectonic deformation has largely ceased, its consequences can be easily overlooked in actively extending settings, like the central Apennines, where the combination of active fault development, Quaternary climatic oscillations and regional uplift already produce a spectacular landscape evolution.

Declaration of competing interest

Acknowledgements

Supplementary Materials

Supplementary data to this article can be found online at https://doi.org/10.1016/j.geomorph.2019.107013.

References

Allen, P.A., Allen, J.R., 2013. Basin Analysis – Principles and Application to Petroleum Play Assessment. third ed. Wiley-Blackwell, Oxford.

Artoni, A., 2013. The Pliocene-Pleistocene stratigraphic and tectonic evolution of the Central sector of the Western Periadriatic Basin of Italy. Marine Petrol. Geol. 42, 82–106.

Ascione, A., Cinque, A., Miccadei, E., Villani, F., Berti, C., 2008. The Plio-Quaternary uplift of the Apennine chain: new data from the analysis of topography and river valleys in Central Italy. Geomorphology 102, 105–118.

Bartolini, C., D'Agostino, N., Dramis, F., 2003. Topography, exhumation, and drainage network evolution of the Apennines. Episodes 26, 212–216.

Bell, R.E., Duclaux, G., Nixon, C.W., Gawthorpe, R.L., McNeill, L.C., 2018. High-angle, not low-angle, normal faults dominate early rift extension in the Corinth Rift, central Greece. Geology 46 (2), 115–118.

Bishop, P., 1995. Drainage rearrangement by river capture, beheading and diversion. Progr. Physic. Geogr. 19, 449–473.

Bogaart, P., Tucker, G., De Vries, J., 2003. Channel network morphology and sediment dynamics under alternating periglacial and temperate regimes: a numerical simulation study. Geomorphology 54, 257–277.

Bosi, C., Galadini, F., Giaccio, B., Messina, P., Sposato, A., 2003. Plio-Quaternary continental deposits in the Latium-Abruzzi Apennines: the correlation of geological events across different intermontane basins. Il Quaternario - Italian. J. Quat. Sci. 16, 55–76.

Bosi, C., Messina, P., Moro, M., 2004. Use of allo-morphosequential units in the Quaternary geological map of the upper Aterno Valley (Central Apennines). Pasquarè G., Venturini C. (Eds.), Mapping geology in Italy, APAT-SELCA.

Cantalamessa, G., Di Celma, C., 2004. Sequence response to syndepositional regional uplift: insights from high-resolution sequence stratigraphy of late Early Pleistocene strata, Periadriatic Basin, central Italy. Sediment. Geol. 164, 283–309.

Cavinato, G.P., DeCelles, P.G., 1999. Extensional basins in tectonically bi-modal central Apennines fold-thrust belt, Italy: response to corner flow above a subducting slab in retrograde motion. Geology 27, 955–958.

Cavinato, G.P., Miccadei, E., 2000. Pleistocene carbonate lacustrine deposits: Sulmona Basin (Central Apennines, Italy). In: Gierlowski-Kordesch, E.H., Kelts, K.R. (Eds.), Lake Basins through Space and Time. 46, pp. 517–526 AAPG Studies in Geology.

Cavinato, G.P., Cosentino, D., De Rita, D., Funiciello, R., Parotto, M., 1993. Tectonic-Sedimentary Evolution of Intrapenninic Basins and Correlation with the Volcano-Tectonic Activity in Central Italy. Mem. Descr. Carta Geol. d'Italia, XLIX, 63–76.

Cavinato, G.P., Gliozzi, E., Mazzini, I., 2000. Two lacustrine episodes during the Late Pliocene-Holocene evolution of the Rieti basin (Central Apennines, Italy), in: Gierlowski-Kordesch, E.H., Kelts, K.R. (Eds.), Lake basins through space and time. AAPG Stud. Geol. 46, 527–534.

Cavinato, G.P., Carusi, C., Dall'Asta, M., Miccadei, E., Piacentini, T., 2002. Sedimentary and tectonic evolution of Plio-Pleistocene alluvial and lacustrine deposits of Fucino Basin (central Italy). Sediment. Geol. 148, 29–59.

Centamore, E., Nisio, S., 2003. Effects of uplift and tilting in the Central-Northern Apennines (Italy). Quat. Internat. 102-102, 93–101.

Chiarini, E., La Posta, E., Cifelli, F., D'Ambrogi, C., Eulilli, V., Ferri, F., Marino, M., Mattei, M., Puzzilli, L.M., 2014. A multidisciplinary approach to the study of the Montereale Basin (Central Apennines, Italy). Rend. Fis. Acc. Lincei 25, S177–S188.

Cohen, K.M., Gibbard, P.L., 2010. Global chronostratigraphical correlation table for the last 2.7 million years v. 2010. Subcommission on Quaternary Stratigraphy, International Commission on Stratigraphy: Cambridge. http://www.quaternary.stratigraphy.org.uk/charts/.

Connell, S.D., Hawley, J.W., Love, D.W., 2005. Late Cenozoic drainage development in the southeastern Basin and Range of New Mexico, southeasternmost Arizona, and western Texas. In: Lucas, S., Morgan, G., Zeigler, K. (Eds.), New Mexico's Ice Ages. 28, pp. 125–150 New Mexico Museum of Natural History and Science Bulletin no.

Cosentino, D., Asti, R., Nocentini, M., Gliozzi, E., Kotsakis, T., Mattei, M., Esu, D., Spadi, M., Tallini, M., Cifelli, F., Pennacchioni, M., Cavuoto, G., Di Fiore, V., 2017. New insights into the onset and evolution of the central Apennine extensional intermontane basins based on the tectonically active L'Aquila Basin (central Italy). Geol. Soc. of America Bulletin 129. https://doi.org/10.1130/B31679.1.

Cowie, P.A., Roberts, G.P., 2001. Constraining slip rates and spacings for active normal faults. J. Struct. Geol. 23, 1901–1915.

Cowie, P.A., Attal, M., Tucker, G.E., Whittaker, A.C., Naylor, M., Ganas, A., Roberts, G.P., 2006. Investigating the surface process response to fault interaction and linkage using a numerical modelling approach. Basin Res. 18, 231–266.

Cowie, P.A., Phillips, R.J., Roberts, G.P., McCaffrey, K., Zijerveld, L.J.J., Gregory, L.C., Faure Walker, J., Wedmore, L.N.J., Dunai, T.J., Binnie, S.A., Freeman, S.P.H.T., Wilcken, K., Shanks, R.P., Huismans, R.S., Papanikolaou, I., Michetti, A.M., Wilkinson, M., 2017. Orogen-scale uplift in the central Italian Apennines drives episodic behaviour of earthquake faults. Nature Sci. Rep. 7, 44858.

D'Anastasio, E., De Martini, P.M., Selvaggi, G., Pantosti, D., Marchioni, A., Maseroli, R., 2006. Short-term vertical velocity field in the Apennines (Italy) revealed by geodetic leveling data. Tectonophysics 418, 219–234.

D'Agostino, N., Jackson, J.A., Dramis, F., Funiciello, R., 2001. Interactions between mantle upwelling, drainage evolution and active normal faulting: an example from the central Apennines (Italy). Geophys. J. Internat. 147, 475–497.

D'Agostino, N., Mantenuto, S., D'Anastasio, E., Giuliani, R., Mattone, M., Calcaterra, S., Gambino, P., Bonci, L., 2011. Evidence for localized active extension in the central Apennines (Italy) from global positioning system observations. Geology 39 (4), 291–294.

De Gelder, G., Fernandez-Blanco, D., Melnick, D., Duclaux, G., Bell, R.E., Jara-Munoz, J., Armijo, R., Lacassin, R., 2019. Lithospheric flexure and rheology determined by climate cycle markers in the Corinth Rift. Nat. Sci. Rep. 9 (1), 4260.

Dickinson, W.R., 2015. Integration of the Gila River drainage system through the Basin and Range province of southern Arizona and southwestern New Mexico (USA). Geomorphology 236, 1–24.

Douglass, J., Meek, N., Dorn, N.I., Schmeekle, M.W., 2009. A criteria-based methodology for determining the mechanism of transverse drainage development, with application to the southwestern United States. GSA Bull. 121, 586–598.

Duffy, O.B., Brocklehurst, S.H., Gawthorpe, R.L., Leeder, M.R., Finch, E., 2015. Controls on landscape and drainage evolution in regions of distributed normal faulting: Perachora Peninsula, Corinth Rift, Central Greece. Basin Res. 27, 473–494.

Faccenna, C., Becker, T.W., Miller, M.S., Serpelloni, E., Willett, S.D., 2014. Isostasy, dynamic topography, and the elevation of the Apennines of Italy. Earth Planet. Sci. Lett. 407, 163–174.

Faure Walker, J.P., 2010. Mechanics of Continental Extension from Quaternary Strain Fields in the Italian Apennines. PhD thesis, University College London, UK, p. 379.

Faure Walker, J.P., Roberts, G.P., Cowie, P.A., Papanikolaou, I., Michetti, A.M., Sammonds, P., Wilkinson, M., McCaffrey, K.J., Phillips, R.J., 2012. Relationship between topography and strain rate in the actively extending Italian Apennines. Earth Planet. Sci. Lett. 325-326, 76–84.

Galadini, F., Galli, P., 2000. Active tectonics in the Central Apennines (Italy) - input data for seismic hazard assessment. Nat. Hazards 22, 225–270.

Galli, P., Giacco, B., Messina, P., 2010. The 2009 central Italy earthquake seen through 0.5 Myr-long tectonic history of the L'Aquila faults system. Quat. Sci. Rev. 29, 3768–3789.

Galli, P., Giacco, B., Messina, P., Peronace, E., Giovanni, M.Z., 2011. Palaeoseismology of the L'Aquila faults (central Italy, 2009, Mw 6.3 earthquake): implications for active fault linkage. Geophys. J. Internat. 187, 1119–1134.

Garcia-Castellanos, D., Verges, J., Gaspar-Escribano, J., Cloetingh, S., 2003. Interplay between tectonics, climate, and fluvial transport during the Cenozoic evolution of the Ebro basin (NE Iberia). J. Geophys. Res. 108, B7.

Gawthorpe, R.L., Leeder, M.R., 2000. Tectono-sedimentary evolution of active extensional basins. Basin Res. 12, 195–218.

Gawthorpe, R.L., Fraser, A.J., Collier, R.E., 1994. Sequence stratigraphy in active extensional basins: implications for the interpretation of ancient basin-fills. Mar. Pet. Geol. 11 (6), 642–658.

Gawthorpe, R.L., Leeder, M.R., Kranis, H., Skourtsos, E., Andrews, J.E., Henstra, G.A., Mack, G.H., Muravchik, M., Turner, J.A., Stamatakist, M., 2018. Tectono-sedimentary evolution of the Plio-Pleistocene Corinth rift, Greece. Basin Res. 30, 448–479.

Geurts, A.H., Cowie, P.A., Duclaux, G., Gawthorpe, R.L., Huismans, R.S., Pedersen, V.K., Wedmore, L.N.J., 2018. Drainage integration and sediment dispersal in active continental rifts: a numerical modelling study of the central Italian Apennines. Basin Res. 30 (5), 965–989.

Giaccio, B., Messina, P., Sposato, A., Voltaggio, M., Zanchetta, G., Galadini, F., Gori, S., Santacroce, R., 2009. Tephra layers from Holocene lake sediments of the Sulmona Basin, central Italy: Implications for volcanic activity in Peninsular Italy and tephrostratigraphy in the central Mediterranean area. Quat. Sci. Rev. 28, 2710–2733.

Giaccio, B., Galli, P., Messina, P., Peronace, E., Scardia, G., Sottili, G., Sposato, A., Chiarini, E., Jicha, B., Silvestri, S., 2012. Fault and basin depocentre migration over the last 2 Ma in the L'Aquila 2009 earthquake region, central Italian Apennines. Quat. Sci. Rev. 56, 69–88.

Giaccio, B., Castorina, F., Nomade, S., Scardia, G., Voltaggio, M., Sagnotti, L., 2013. Revised Chronology of the Sulmona Lacustrine Succession, Central Italy. J. Quat. Sci. 28, 545–551.

Giraudi, C., 1989. Lake levels and climate for the last 30,000 years in the Fucino area (Abruzzo-central Italy) – a review. Palaeogeogr., Palaeoclim., Palaeoecol. 70, 249–260.

Giraudi, C., Frezzotti, M., 1997. Late Pleistocene glacial events in the central Apennines, Italy. Quat. Res. 48, 280–290.

Gliozzi, E., Mazzini, I., 1998. Palaeoenvironmental analysis of Early Pleistocene brackish marshes in the Rieti and Tiberino intrapenninic basins (Latium and Umbria, Italy) using ostracods (Crustacea). Palaeogeogr., Palaeoclimat. Palaeoecol. 140, 325–333.

Gori, S., Falcucci, E., Scardia, G., Nomade, S., Guillou, H., Galadini, F., Fredi, P., 2015. Early capture of a central Apennine (Italy) internal basin as a consequence of enhanced regional uplift at the Early-Middle Pleistocene transition. In: Monegato, G., Gianotti, F., Forno, M.G. (Eds.), The Plio-Pleistocene Continental Record in Italy: Highlights on Stratigraphy and Neotectonics. Abstracts Volume AIQUA Congress 2015, February 24–26, Torino, Miscellanea dell'Istituto Nazionale di Geofisica e Vulcanologia (ISSN 2039–6651). 26, pp. 26–27.

Gori, S., Falcucci, E., Ladina, C., Marzorati, S., Galadini, F., 2017. Active faulting, 3-D geological architecture and Plio-Quaternary structural evolution of extensional basins in the central Apennine chain, Italy. Solid Earth 8, 319–337.

Head, M.J., Gibbard, P.L., 2015. Early-Middle Pleistocene transitions: linking terrestrial and marine realms. Quat. Internat. 389, 7–46.

House, P.K., Pearthree, P.A., Perkins, M.E., 2008. Stratigraphic evidence for the role of lake spillover in the inception of the lower Colorado River in southern Nevada and western Arizona. In: Reheis, M.C., Hershler, R., Miller, D.M. (Eds.), Late Cenozoic Drainage History of the Southwestern Great Basin and Lower Colorado River Region: Geological and Biotic Perspectives. 439, pp. 335–353 Geol. Soc. of America Special Paper.

Jackson, J., Leeder, M., 1994. Drainage Systems and the Development of Normal Faults - an example from Pleasant Valley, Nevada. J. Struct. Geol. 16, 1041–1059.

Jost, A., Lunt, D., Kageyama, M., Abe-Ouchi, A., Peyron, O., Valdes, P.J., Ramstein, G., 2005. High-resolution simulations of the last glacial maximum climate over Europe: a solution to discrepancies with continental palaeoclimatic reconstructions? Clim. Dyn. 24, 577–590.

Kettner, A.J., Syvitski, J.P.M., 2008. Predicting discharge and sediment flux of the Po River, Italy since the last Glacial Maximum, in: De Boer, P.L., Postma, G., Van der Zwan, C., Burgess, P.M., Kukla, P.A. (Eds.), Analogue and Numerical Forward Modelling of Sedimentary Systems: From Understanding to Prediction. Int. Assoc. of Sedimentol. Spec. Publ. vol. 40, pp. 171–190.

Larson, P.H., Dorn, R.I., Palmer, R.E., Bowles, Z., Harrison, E., Kelley, S., Schmeeckle, M.W., Douglass, J., 2014. Pediment response to drainage basin evolution in south-central Arizona. Phys. Geogr. 35 (5), 369–389. https://doi.org/10.1080/02723646.2014.931089.

Larson, P.H., Meek, N., Douglass, J., Dorn, R.I., Seong, Y.B., 2017. How rivers get across mountains: transverse drainages. Annals Am. Assoc. Geograph. 107 (2), 274–283.

Lastoria, B., Miserocchi, F., Lanciani, A., Monacelli, G., 2008. An estimated erosion map for the Aterno-Pescara river basin. European Water 21-22, 29–39.

Lavecchia, G., Brozzetti, F., Barchi, M., Menichetti, M., Keller, J.V.A., 1994. Seismotectonic zoning in east-central Italy deduced from an analysis of the Neogene to present deformations and related stress fields. Geol. Soc. America Bull. 106, 1107–1120.

Lavecchia, G., Ferrarini, F., Brozzetti, F., De Nardis, R., Boncio, P., Chiaraluce, L., 2012. From surface geology to aftershock analysis: constraints on the geometry of the L'Aquila 2009 seismogenic fault system. Ital. J. Geosci. 131 (3), 330–347.

Loget, N., Van Den Driessche, J., 2009. Wave train model for knickpoint migration. Geomorphology 106, 376–382.

Lombardo, M., Calderoni, G., D'Alessandro, L., Miccadei, E., 2001. The travertine deposits of the Upper Pescara Valley (Central Abruzzi, Italy): a clue for the reconstruction of the Late Quaternary palaeoenvironmental evolution of the area. In: Visconti, G., Beniston, M., Iannorelli, E.D., Barba, D. (Eds.), Global Change and Protected Areas. Advances in Global Change Research. 9. Springer, Dordrecht.

Macri, P., Smedile, A., Speranza, F., Sagnotti, L., Porreca, M., Mochales, T., Russo Ermolli, E., 2016. Analysis of a 150 m sediment core from the co-seismic subsidence depocenter of the 2009 Mw = 6.1 L'Aquila earthquake (Italy): Implications for Holocene-

Pleistocene tectonic subsidence rates and for the age of the seismogenic Paganica fault system. Tectonophysics 687, 180–194.

Magni, V., Faccenna, C., Van Hunen, J., Funiciello, F., 2014. How collision triggers backarc extension: Insight into Mediterranean style of extension from 3-D numerical models. Geology 42, 511–514.

Magri, D., Di Rita, F., Palombo, M.R., 2010. An Early Pleistocene interglacial record from an intermontane basin of central Italy (Scoppito, L'Aquila). Quat. Internat. 225, 106–113.

Mancini, M., D'Anastasio, E., Barbieri, M., De Martini, P.M., 2007. Geomorphological, paleontological and $^{87}Sr/^{86}Sr$ isotope analyses of early Pleistocene paleoshorelines to define the uplift of Central Apennines (Italy). Quat. Res. 67, 487–501.

Mancini, M., Cavuoto, G., Pandolfi, L., Petronio, C., Salari, L., Sardella, R., 2012. Coupling basin infill history and mammal biochronology in a Pleistocene intramontane basin: the case of western L'Aquila Basin (central Apennines, Italy). Quat. Int. 267, 62–77.

Meek, N., 1989. Geomorphic and hydrologic implications of the rapid incision of Afton Canyon, Mojave Desert. Calif. Geol. 17, 7–10.

Meek, N., 2019. Episodic forward prolongation of trunk channels in the Western United States. Geomorphology 340, 172–183.

Menges, C.M., 2008. Multistage late Cenozoic evolution of the Amargosa River drainage, southwestern Nevada and eastern California. In: Reheis, M.C., Hershler, R., Miller, D. M. (Eds.), Late Cenozoic Drainage History of the Southwestern Great Basin and Lower Colorado River Region: Geological and Biotic Perspectives. Geol. Soc. of America Special Paper. 439, pp. 39–90.

Miccadei, E., Piacentini, T., Barberi, R., 2002. Uplift and local tectonic subsidence in the evolution of intramontane basins: the example of the Sulmona basin (central Apennines, Italy). Studi Geol. Camerti 119–133.

Montone, P., Mariucci, M.T., Pondrelli, S., Amato, A., 2004. An improved stress map for Italy and surrounding regions (Central Mediterranean). J. Geophys. Res. 109, B10410.

Moro, M., Gori, S., Falcucci, E., Saroli, M., Galadini, F., Salvi, S., 2013. Historical earthquakes and variable kinematic behaviour of the 2009 L'Aquila seismic event (central Italy) causative fault, revealed by paleoseismological investigations. Tectonophysics 583, 131–144.

Nocentini, M., Asti, R., Cosentino, D., Durante, F., Gliozzi, E., Macerola, L., Tallini, M., 2017. Plio-Quaternary geology of L'Aquila-Scoppito Basin (Central Italy). J. Maps 13 (2), 563–574.

Nocentini, M., Cosentino, D., Spadi, M., Tallini, M., 2018. Plio-Quaternary geology of the Paganica-San Demetrio-Castelnuovo Basin (Central Italy). J. Maps 14 (2), 411–420.

Palombo, M.R., Mussi, M., Agostini, S., Barbieri, M., Di Canzio, E., Di Rita, F., Fiore, I., Iacumin, P., Magri, D., Speranza, F., Tagliacozzo, A., 2010. Human peopling of Italian intramontane basins: the early Middle Pleistocene site of Pagliare di Sassa (L'Aquila, central Italy). Quat. Internat. 223-224, 170–178.

Patacca, E., Sartori, R., Scandone, P., 1990. Tyrrhenian Basin and Apenninic Arcs: kinematic relations since late Tortonian times. Mem. Soc. Geol. It. 45, 425–451.

Phillips, F.M., 2008. Geological and hydrological history of the paleo-Owens River drainage since the late Miocene. In: Reheis, M.C., Hershler, R., Miller, D.M. (Eds.), Late Cenozoic Drainage History of the Southwestern Great Basin and Lower Colorado River Region: Geological and Biotic Perspectives. 439, pp. 115–150 Geol. Soc. of America Special Paper.

Piacentini, T., Miccadei, E., 2014. The role of drainage systems and intermontane basins in the Quaternary landscape of the Central Apennines chain (Italy). Rend. Fis. Acc. Lincei 25, S139–S150.

Pizzi, A., 2003. Plio-Quaternary uplift rates in the outer zone of the central Apennines fold-and-thrust belt, Italy. Quat. Internat. 101–102, 229–237.

Porreca, M., Smedile, A., Speranza, F., Mochales, T., Caracciolo, F.D., Di Giulio, G., Vassallo, M., Villani, F., Nicolosi, I., Carluccio, R., Amoroso, S., Macri, P., Buratti, N., Durante, F., Tallini, M., Sagnotti, L., 2016. Geological reconstruction in the area of maximum co-seismic subsidence during the 2009 Mw=6.1 L'Aquila earthquake using geophysical and borehole data. Ital. J. Geosci. 135, 350–362.

Pucci, S., Villani, F., Civico, R., Pantosti, D., Del Carlo, P., Smedile, A., DeMartini, P.M., Pons-Branchu, E., Gueli, A., 2015. Quaternary geology of the Middle Aterno Valley, 2009 L'Aquila earthquake area (Abruzzi Apennines, Italy). J. Maps 11:5, 689–697.

Ramrath, A., Zolitschka, B., Wulf, S., Negendank, J.F.W., 1999. Late Pleistocene climatic variations as recorded in two Italian maar lakes (Lago di Mezzano, Lago Grande di Monticchio). Quat. Sci. Rev. 18, 977–992.

Reheis, M.C., Adams, K.D., Oviatt, C.G., Bacon, S.N., 2014. Pluvial lakes in the Great Basin of the western United States – a view from the outcrop. Quat. Sci. Rev. 97, 33–57.

Repasch, M., Karlstrom, K., Heizler, M., Pecha, M., 2017. Birth and evolution of the Rio Grande fluvial system in the past 8 Ma: progressive downward integration and the influence of tectonics, volcanism, and climate. Earth-Science Rev. 168, 113–164.

Roberts, G.P., Michetti, A.M., 2004. Spatial and temporal variations in growth rates along active normal fault systems: an example from Lazio-Abruzzo, central Italy. J. Struct. Geol. 26, 339–376.

Roda-Boluda, D.C., Whittaker, A.C., 2016. Normal fault evolution and coupled landscape response: examples from the Southern Apennines, Italy. Basin Res. 30 (1), 186–209.

Roda-Boluda, D.C., Whittaker, A.C., 2017. Structural and geomorphological constraints on active normal faulting and landscape evolution in Calabria, Italy. J. Geol. Soc. Lond. 174, 701–720.

Royden, L.H., 1993. The tectonic expression slab pull at continental convergent boundaries. Tectonics 12 (2), 303–325.

Santo, A., Ascione, A., Di Crescenzo, G., Miccadei, E., Piacentini, T., Valente, E., 2014. Tectonic-geomorphological map of the middle Aterno River valley (Abruzzo, Central Italy). J. Maps 10:3, 365–378.

Serpelloni, E., Faccenna, C., Spada, G., Dong, D., Williams, S.D.P., 2013. Vertical GPS ground motion rates in the Euro-Mediterranean region: new evidence of velocity gradients at

different spatial scales along the Nubia-Eurasia plate boundary. J. Geophys. Res. Solid Earth 118, 1–22.

Stock, J.D., Montgomery, D.R., 1999. Geologic constraints on bedrock river incision using the stream power law. J. Geophys. Res. 104, 4983–4993.

Tarquini, S., Isola, I., Favalli, M., Mazzarini, F., Bisson, M., Pareschi, M.T., Boschi, E., 2007. TINITALY/01: a new Triangular Irregular Network of Italy. Ann. Geophys. 50, 407–425.

Tucker, G.E., McCoy, S.W., Whittaker, A.C., Roberts, G.P., Lancaster, S.T., Phillips, R., 2011. Geomorphic significance of postglacial bedrock scarps on normal-fault footwalls. J. Geophys. Res. 116, F01022.

Vezzani, L., Ghisetti, F.C., 1998. Carta Geologica dell'Abruzzo: Scala 1:100.000. Selca, Firenze, Italy.

Vezzani, L., Festa, A., Ghisetti, F.C., 2010. Geology and tectonic evolution of the Central-Southern Apennines, Italy. Geol. Soc. of America Spec. Paper 469, 58.

Wegmann, K.W., Pazzaglia, F.J., 2009. Late Quaternary fluvial terraces of the Romagna and Marche Apennines, Italy: climatic, lithologic, and tectonic controls on terrace genesis in an active orogeny. Quat. Sci. Rev. 28, 137–165.

Whittaker, A.C., Boulton, S.J., 2012. Tectonic and climatic controls on knickpoint retreat rates and landscape response times. J. Geophys. Res. 117, F02024.

Whittaker, A.C., Cowie, P.A., Attal, M., Tucker, G.E., Roberts, G.P., 2007. Contrasting transient and steady-state rivers crossing active normal faults: new field observations from the Central Apennines, Italy. Basin Res. 19, 529–556.

Whittaker, A.C., Attal, M., Cowie, P.A., Tucker, G.E., Roberts, G.P., 2008. Decoding temporal and spatial patterns of fault uplift using transient river long-profiles. Geomorphology 100, 506–526.

Whittaker, A.C., Attal, M., Allen, P.A., 2010. Characterising the origin, nature and fate of sediment exported from catchments perturbed by active tectonics. Basin Res. 22, 809–828.

Wu, H., Guiot, J., Brewer, S., Guo, Z., 2007. Climatic changes in Eurasia and Africa at the last glacial maximum and mid-Holocene: reconstruction from pollen data using inverse vegetation modelling. Clim. Dyn. 29, 211–229.

Zanchetta, G., Bini, M., Giaccio, B., Manganelli, G., Benocci, A., Regattieri, E., Colonese, A.C., Boschi, C., Biagioni, C., 2017. Middle Pleistocene (MIS14) environmental conditions in the central Mediterranean derived from terrestrial molluscs and carbonate stable isotopes from Sulmona Basin (Italy). Palaeogeogr. Palaeoclim. Palaeoecol. 485, 236–246.